Aus der Medizinische Klinik m.S. Gastroenterologie, Infektiologie und Rheumatologie der Charité - Universitätsmedizin Berlin

DISSERTATION

Tumor-Stroma Crosstalk in Colorectal Cancer: The Role of Paracrine Hedgehog Signaling

zur Erlangung des akademischen Grades

Doctor medicinae (Dr. med.)

vorgelegt der Medizinischen Fakultät

Charité – Universitätsmedizin Berlin

von

Leonard Marcel Kirn

aus Marburg

Datum der Promotion: 13.12.2019

0 Introductory Remarks

The results presented herein were in parts published in:

Marco Gerling, Nike V.J.A. Büller*, Leonard M. Kirn*, Simon Joost, Oliver Frings, Benjamin Englert, Åsa Bergström, Raoul V. Kuiper, Leander Blaas, Mattheus C.B. Wielenga, Sven Almer, Anja A. Kühl, Erik Fredlund, Gijs R. van den Brink & Rune Toftgård (2016). *Stromal Hedgehog signalling is downregulated in colon cancer and its restoration restrains tumour growth*. Nature Communications *7*, 12321; doi:10.1038/ncomms12321; * equal contribution

Index

Tables

Figures

1 Abstract

1.1 Abstract (English)

Introduction

Colorectal cancer (CRC) is one of the most common malignancies worldwide. The role of the Hedgehog (Hh) signaling pathway in CRC is controversial. Based on previous data suggesting either a paracrine or autocrine tumor-supportive role for Hh, a clinical trial with a specific Hh inhibitor was conducted, but yielded a negative result. The aim of this study was to elucidate the role of Hh signaling in the development and progression of CRC based on CRC mouse models.

Methods

The role of Hh signaling in tumor-stroma crosstalk was analyzed based on chemically induced inflammation-driven and sporadic tumor models that were combined with different genetically modified mouse strains. By applying immunohistochemistry (IHC) and real-time quantitative polymerase chain reaction (RT-qPCR) in combination with Hh reporter mice, we investigated the activation of the Hh pathway in murine colonic tumors. Furthermore, we used microarray technology for gene expression analysis in mice with genetic activation of the Hh pathway. Additionally, we analyzed gene expression data sets of murine or human stromal cells treated with Hh ligands *in vitro*.

Results

Hh reporter mice revealed that downstream Hh signaling remains stromal in murine colonic tumors and that the canonical Hh pathway is down-regulated during tumorigenesis.

Transgenic mice with activated Hh signaling in stromal cells showed reduced tumor burden in both tumor models. In further support of a protective effect of the Hh pathway in CRC, we found down-regulation of the tumor-promoting epithelial transcription factor PROX1 upon genetic Hh activation in the stroma.

Bone morphogenetic protein (BMP) signaling acts as a differentiation factor in the intestinal epithelium and is regulated by Hh signaling. Analysis of epithelial p-SMAD1/5 expression, a readout of active BMP signaling, revealed an association of Hh activity in the stroma with increased BMP pathway activity in the adjacent epithelial compartment. Gene expression data suggested that stromal Hh activation diminishes BMP inhibitor expression. Finally, analysis of

gene expression in fibroblasts treated with Hh ligand *in vitro* confirmed down-regulation of BMP inhibitor expression upon activation of Hh signaling in intestinal stromal cells.

Conclusion

Together, the results suggest a tumor-protective role of stromal Hh activation on CRC formation in mice, which may partly be achieved through alterations in the Hh-BMP axis.

1.2 Zusammenfassung

Einleitung

Das kolorektale Karzinom (CRC) ist einer der häufigsten Tumore weltweit. Die Rolle des Hedgehog (Hh) Signalweges für die Pathogenese des CRC ist umstritten. Basierend auf früheren Daten, welche eine parakrine oder autokrine protumorigene Rolle des Hh Signalweges nahelegten, ist eine klinische Studie mit einem spezifischen Hh Inhibitor durchgeführt worden, die jedoch keinen positiven Effekt der Hh Inhibition nachweisen konnte. Das Ziel dieser Studie war es daher, die Rolle des Hh Signalweges in der Entstehung und Entwicklung vom CRC in Mausmodellen zu untersuchen.

Methodik

Ein durch die Applikation von chemischen Karzinogenen hervorgerufenes Entzündungs-abhängiges sowie ein sporadisches CRC Tumormodell wurden in Kombination mit verschiedenen transgen veränderten Mausstämmen genutzt, um die Rolle des Hh Signalweges in Wechselspiel zwischen Tumor und Stroma zu analysieren. Mit Hilfe von Immunhistochemie (IHC) und quantitativer Echtzeit-PCR (RT-qPCR) in Kombination mit Hh Reportermäusen wurde die Expression des Hh Signalweges in murinen Kolontumoren untersucht. Für Genexpressionsanalysen wurde die Microarray Technologie an Mäusen mit genetisch induzierter Hh-Aktivierung angewandt. Zusätzlich wurden Genexpressionsdatensätze, in denen murine und humane stromale Zellen *in vitro* mit Hh Liganden behandelt wurden, hinsichtlich der Expression von Hh-regulierten Genen untersucht.

Ergebnisse

Wir konnten zeigen, dass die Aktivierung des „kanonischen“ Hh Signalweges in murinen Kolontumoren auf das Stroma beschränkt ist und dass Hh Zielgene herunterreguliert sind. Mäuse mit Aktivierung von Hh in stromalen Zellen zeigten eine verminderte Tumorlast. Weiterhin konnten wir zeigen, dass es nach Aktivierung von Hh zu einer Runterregulierung des protumorigenen Transkriptionsfaktors PROX1 kommt. Der „bone morphogenetic protein“ (BMP) Signalweg hatte eine pro-differenzierende Rolle im Epithel und wurde durch Hh Signale gesteuert.

IHC für p-SMAD1/5, welche die Aktivierung des BMP Signalweges signalisieren, zeigte, dass die Aktivität von Hh im Stroma mit erhöhten BMP Signalen im Epithelium einhergeht. In der Genexpressionsanalyse zeigte sich, dass stromale Hh Aktivierung die Expression von BMP Inhibitoren vermindert, welches sich in der Analyse von Genexpressionsmuster in intestinalen Fibroblasten *in vitro* bestätigte.

Schlussfolgerung

Zusammenfassend zeigen unsere Ergebnisse, dass stromale Hh Aktivierung eine protektive Rolle auf die Entstehung von CRC in Mausmodellen ausübt, die zumindest in Teilen durch die Hh-BMP Achse vermittelt wird.

2 Introduction

2.1 Histology of the intestine

2.1.1 Overview

The intestine is comprised of the small intestine and the colon, both of which can be further subdivided anatomically. Macroscopically, the small intestine consists of three major parts, the duodenum, jejunum, and ileum. The large intestine consists of the caecum, colon, and rectum. Histologically, the intestinal tract is a three-layered tube [1]. Its outer layer, *tunica muscularis*, consists mainly of innervated smooth muscle cells, which orchestrate intestinal peristalsis. The middle layer, the submucosa, contains a diverse stromal cell population, vessels and lymphatic lacteals [2]. The mucosa, the inner layer, consists of the epithelium, the *lamina propria*, and the *muscularis mucosae* [3].

The small intestine

The absorptive surface of the small intestine is significantly increased by projections (villi) and invaginations towards the submucosa, termed the crypts of Lieberkühn [1]. The small intestinal epithelium consists of at least four differentiated cell types: enterocytes, whose main task is nutrient absorption; mucus-secreting goblet cells; rare enteroendocrine cells, which produce hormones such as serotonin, substance P, and secretin [1]; and in the small intestine specifically, an additional cell type exists at the bottom of the crypts, called Paneth cells, which produces antimicrobial peptides and enzymes such as cryptidins/defensins, and lysozyme, playing a key role in innate immunity [1].

The large intestine

The main function of the large intestine is the absorption of water and electrolytes. In humans, its diameter reaches almost twice that of the small intestine, while it is only one third as long [4]. The colonic mucosa differs in its composition from the mucosa of the small intestine in that it lacks villi and is comprised of crypts only [1]. In contrast to the small intestinal epithelium, the large intestinal epithelium lacks Paneth cells [5]. In addition, the colon contains fewer enteroendocrine cells, but more goblet cells. The bottom of the crypt builds a niche for epithelial stem cells [6].

2.1.2 The intestinal stroma

"Stroma" can be defined as the supporting surroundings of an organ, which can be subdivided into two major parts: the extracellular matrix (ECM) and the stromal cells [7]. The cellular part is comprised of pericytes, smooth muscle cells, lymphatic pericytes (colon), smooth muscle cells associated with lymphatic lacteals (small intestine), mesenchymal stem cells (MSC), myofibroblasts, fibroblasts, and immune cells [8]. The histological differentiation of these elements is challenging due to the lack of specific markers. Table 1 gives a summary of the major cell types of the intestinal stroma and three selected markers used to identify the different components. These markers,α-sma, desmin and vimentin, are all intracellular proteins of the cytoskeleton [9].

	α-SMA	Desmin	Vimentin
Myofibroblast	+	-	+
Fibroblast	-	-	+
Pericyte	+	+/-	+
Mesenchymal stem cell	+	-	+
Smooth muscle cell	+*	+	-

Table 1. Immunhistological markers of stromal cell types. α-SMA = α-smooth muscle actin
Rows represent cell types, columns represent markers. *negative if precursor cell [10]

Briefly, pericytes (vascular smooth muscle cells) are capillary-associated contractile cells that contribute to angiogenesis and revascularization via paracrine signals [9]. Smooth muscle cells build up the *lamina muscularis mucosae* and the *tunica muscularis*, which consists of outer longitudinal and inner circular smooth muscle cells [2]. MSCs are multipotent cells that can differentiate into several different cell types, including osteoblasts, chondrocytes, adipocytes, tenocytes, myocytes, and neural cells [11]. Fibroblasts, spindle-shaped cells, produce collagens, hyaluronic acid, proteoglycans and fibronectins, substances which together form the ECM [12]. Myofibroblasts are so-called "activated" fibroblasts that express proteins such as α-smooth muscle actin (α-SMA), contractile stress fibers and fibronectins [13,14]. Myofibroblasts are activated by injury and during tumor development, where they adopt a crucial role in the control of epithelial proliferation and differentiation processes as outlined below. Furthermore, in conjunction with other stromal cells, they contribute to the complex gastrointestinal immune response [9]. While the exact origin of

myofibroblasts remains elusive, they have been shown to either stem from resident fibroblasts, stellate cells, MSCs, perivascular smooth muscle cells, or through a transdifferentiation process called epithelial-to-mesenchymal transition from epithelial cells [9] (outlined in more detail in *"Charakterisierung des Tumorstromas im Mausmodell kolorektaler Karzinome"* Leonard M. Kirn, [M23 Hausarbeit, 2015]).

2.2 Developmental pathways in the intestine

Interactions of several signaling pathways are pivotal for correct development and homeostasis of the intestine. Such developmental pathways consist of a number of successive processes that culminate in the expression or repression of specific sets of genes. In the intestine, the three morphogenic signaling pathways, Wnt, bone morphogenetic protein (BMP), and Hedgehog (Hh), are of central importance. Ligands for each of these pathways are found in specific concentrations during development, as well as in the adult intestine in gradients along the crypt(-villous) axis [1] (Figure 1).

2.2.1 Wnt signaling

The Wnt pathway is a main regulator of epithelial proliferation in colonic crypts. Moreover, mutations of Wnt pathway members are regularly found in colorectal cancer (CRC) at early stages [15]. Wnt ligands bind to receptors of the "Frizzled" family; upon binding, downstream signals inhibit a degradation complex, which consists of the tumor suppressors axin and adenomatous polyposis coli (APC). In the absence of Wnt ligands, this complex leads to the degradation of β-catenin, the major downstream effector of the pathway [16].

As a result of Wnt activation, β-catenin protein abundance in the cell increases, and it translocates into the nucleus to activate several transcription factors of the T cell factor/lymphocyte enhancer factor (TCF/LEF) family [5]. As the β-catenin/TCF4 complex acts as a main regulator of cell proliferation and differentiation, its activation in CRC cells promotes cellular proliferation and dedifferentiation [17]. The activation of different transcription factors downstream of the Wnt pathway in the normal colon differs from that in neoplastic colon cells to some extent, as for example the transcription factor prospero homeobox 1 (PROX1), which is thought to promote tumor cell growth, is highly expressed in neoplastic cells, but not in the normal intestine [18].

2.2.2 Bone morphogenetic protein signaling

The BMP pathway acts mainly as an antagonist to the Wnt pathway and supports epithelial differentiation, while suppressing epithelial proliferation [19]. BMPs belong to the transforming growth factor-β (TGFβ) superfamily, in which ligands transduce their signals through phosphorylation processes of serine-threonine kinase receptors [20]. Upon BMP binding to the receptor, a receptor-associated Smad (R-SMAD), either SMAD1, -5, or -8, or a combination of these gets phosphorylated and builds a complex with SMAD4, the only known "common-partner Smad" in mammals [20]. Through diverse mechanisms that include direct binding to the DNA, interaction with transcription factors, and the recruitment of transcriptional coactivators/corepressors, the SMAD dimers regulate the transcription of target genes [20]. Activated BMP signaling is present in differentiated epithelial cells and in the stroma of the *lamina propria*, signified by the presence of phosphorylated R-SMADs (e.g. by immunohistochemistry for p-SMAD1/5) [9].

2.2.3 The Hedgehog pathway

While Wnt signaling drives intestinal stem cell proliferation and plays an important role in CRC, the role of Hh signaling in the intestine is less well defined. There are three active mammalian hedgehog proteins: Sonic Hedgehog (SHH), Indian Hedgehog (IHH), and Desert Hedgehog (DHH), which all consist of an essential 19-kDa NH_2-terminal fragment [21]. The proteins are synthesized as 45-kDa precursors, which are highly processed posttranslationally [21]. The detachment of the lipid-modified Hh proteins from the cell membrane requires the presence of Dispatched (DISP) [3]. After the release, the Hh ligands bind to Patched (PTCH, of which PTCH1 and its isoform PTCH2 exist), a 12-transmembrane receptor, which inhibits another seven-transmembrane protein, smoothened (SMO). The binding of the ligands to PTCH1/2 attenuates the inhibitory effect on SMO, which can then activate signaling intracellularly [3]. As a result of the relief, SMO signals downstream through several kinases, leading to the procession of the three glioma-associated protein homologue (GLI) transcription factors: GLI1, GLI2, and GLI3. GLI1 and GLI2 are mainly processed into activating transcriptional factors, which takes place in the primary cilium, a specific cell organelle [22]. Target genes of this so-called "canonical" cascade include multiple genes such as *PTCH1/2*, *GLI1*, and Hedgehog-interacting protein (*HHIP*), the latter of which acts mainly as a negative regulator of the pathway [21]. In the intestine, the major Hh

ligand is IHH, which is secreted by differentiated enterocytes, while the response is exclusively stromal, as evidenced by stromal expression of GLI1 proteins [23].

The Hh pathway is of major importance for the intestinal development of all bilaterians [21]. This is confirmed by different mouse models with genetic knockouts in Hh pathway genes, which generally results in severe intestinal phenotypes [3]. In the adult intestine, Hh signaling is necessary for the maintenance of the mesenchymal cells of the *lamina propria* [3].

The importance of Hh for mesenchymal homeostasis in the adult intestine was confirmed by several experiments designed to alter the level of Hh activity in adult mice. A change in the myofibroblast composition was shown, since a body-wide loss of *Ptch1* drives myofibroblast accumulation [24]. Reduction of Hh levels, either by expression of a dominant active form of an Hh inhibitor [25] or a specific knockout of *Ihh* in epithelial cells [26], led to progressive myeloid inflammation, loss of differentiated smooth muscle cells and changes in myofibroblast composition. A similar study found that decreased Hh signaling is a main cause for a loss of villus smooth muscle and the *muscularis mucosa* [10]. Moreover, up-regulation of Hh signaling was found to support smooth muscle differentiation [10]. These findings implicate that villus smooth muscle cells are particularly sensitive to Hh signaling.

2.3 Cell renewal and stem cells in the intestinal epithelium - complex interactions of signaling pathways

The intestinal epithelium is one of the fastest self-renewing tissues in adult mammals with a turnover of 3-5 days [6]. The source for this constant epithelial renewal are stem cells located at the crypt base, which can be identified by their expression of leucine-rich repeat-containing G- protein coupled receptor 5 (*Lgr5*) [6]. These *Lgr5*$^{+}$ stem cells in the crypt give rise to transit-amplifying cells. While the transit-amplifying cells move up the crypt, they differentiate into the non-dividing, terminally differentiated enterocytes and most other cell types of the intestinal epithelial such as goblet cells or Paneth cells [27]. The major components that build the intestinal stem cell niche are neighboring epithelial cells (such as Paneth cells in the small intestine and specific goblet cells in the colon [28]), mesenchymal cells (intestinal subepithelial myofibroblasts [ISEMFs]), and proteins of the basement membrane [29].

Epithelial Wnt signaling centrally controls the intestinal stem cell state [5]. While Paneth cells in the crypt bottom were thought to be the main source of Wnt ligands [30], recent data shows that

extraepithelial mesenchymal cells also produce Wnt ligands to sustain the intestinal stem cell niche [31]. On the other hand, intestinal differentiation and inhibition of stem cell activation is supported by mesenchymally derived BMP signals, which antagonize Wnt signaling, resulting in decreased nuclear β-catenin concentrations [9]. The pro-differentiating effects of Hh are not yet fully understood, but as IHH has been shown to drive stromal BMP synthesis [3], it is generally viewed as a negative regulator of epithelial cell proliferation. Consistently, knockout of the main epithelial Hh ligand in the adult small intestine leads to an expansion of the intestinal stem cell compartment and enterocyte dedifferentiation [26]. It has recently been shown that colon crypt myofibroblasts and smooth muscle cells secrete BMP antagonists, such as gremlin 1 (GREM1), gremlin 2 (GREM2), and chordin-like 1 (CRDL1) to protect the intestinal stem cell niche from differentiation through BMPs [32,33]. The Wnt, BMP, and Hh pathways are expressed in gradients along the crypt axis underscoring their individual role in the balance between colonic proliferation and differentiation [34] (Figure 1).

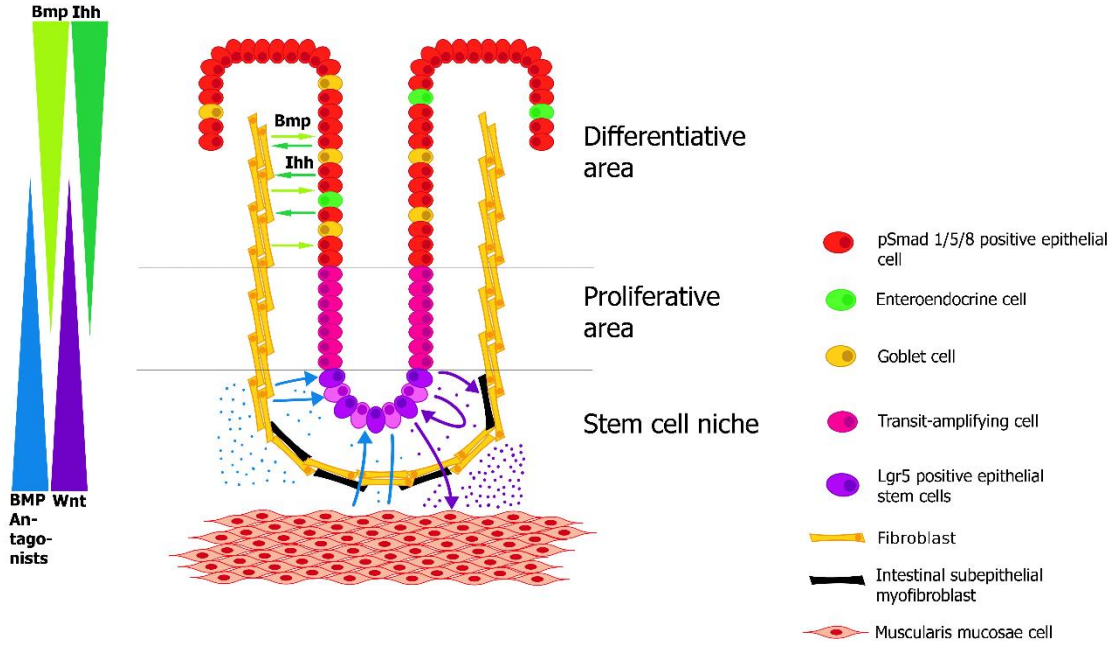

Figure 1. Indian Hedgehog, bone morphogenetic protein, Wnt proteins, and bone morphogenetic protein-antagonist gradient expression in the colonic crypt.

The main Hh ligand in the colon, IHH, is produced by differentiated epithelial cells, while downstream Hh signal transduction is exclusively stromal. Mechanistically, IHH is thought to induce stromal BMP synthesis. BMPs signal towards the epithelium, as indicated by phosphorylated Smads (p-SMAD1/5/8). The BMP pathway promotes differentiation by inhibiting the Wnt pathway, which itself is up-regulated in the bottom of the crypt, together with BMP antagonists that inhibit the effects of BMP signaling, contributing to forming a stem cell niche.

2.4 Colorectal cancer

2.4.1 Epidemiology

CRC is a pervasive malignant disease: it represents the third most common cancer in men worldwide, with 10 % of all new cancer cases in the year 2012, exceeded only by lung (16.7 %) and prostate cancer (15.0 %), and the second most common cancer in women with 9.2 % after breast cancer, which accounts for 25.2 % [35]. CRC causes around 700,000 deaths per year worldwide. There are regional differences in incidence with a peak in Australia and New Zealand and a minimum in Western Africa [35], which might partly be explained genetically, and partly by lifestyle risk factors such as physical inactivity, smoking, obesity, excessive consumption of alcohol and red meat [36]. While the incidence in Germany has continuously increased since 1980, the mortality has declined during the past decades [37]. Improved treatment options as well as earlier detection through a tailored screening program have contributed to this improvement [38]: in 2002, a surveillance program was introduced, which includes an annual fecal occult blood test starting at the age of 50, and a colonoscopy at the age of 55, followed by defined consecutive surveillance intervals.

2.4.2 Staging and treatment

CRC diagnosis is mainly established by rectal examination and colonoscopy. Staging of a newly diagnosed CRC follows a multidisciplinary approach: in Germany specifically, it includes complete colonoscopy, chest radiography, measurement of the tumor marker carcinoembryonic antigen (CEA), an abdominal ultrasound, and a physical examination of the patient. Therapeutic decisions are generally based on tumor stage, and take into account the individual patient's characteristics. The hallmark of CRC therapy is the surgical tumor removal with total resection and lymphadenectomy. The decision about (neo-) adjuvant therapy is based on tumor stage, localization, and the individual characteristics of the patient [39].

2.4.3 Colorectal carcinogenesis and hereditary diseases leading to colorectal cancer

The adenoma-carcinoma sequence (often referred to as the "Vogelstein model") describes a model of colorectal tumorigenesis in which multiple consecutive somatic mutations lead to progression from benign adenomas to carcinomas. Vogelstein *et al*. distinguished the mutated genes into gatekeeper genes, which encode for proteins controlling cell proliferation and differentiation, and caretaker genes which, for example, express genome stabilizing products [40]. More recently, a new

term was coined: landscaper genes; the abnormal expression of these genes does not influence cellular growth directly, but results in a pathologic microenvironment, which supports tumor growth [41].

The consecutive mutations in the genes *KRAS* and *APC* (examples for gatekeeper genes), *tumor protein P53* (example for caretaker function), and *deleted in colorectal carcinoma (DCC*, a potential gatekeeper gene [42]) all play important roles in tumor development [43].

The understanding of the underlying pathomechanisms of genetic diseases that increase the risk for CRC has shed light on some of the basic principles that drive malignant transformation in the colon. Two important hereditary diseases that greatly increase CRC risk are Familial adenomatous polyposis (FAP) and hereditary non-polyposis colorectal cancer (HNPCC or Lynch Syndrome). Lynch syndrome is an autosomal dominant disease, in which about 90 % of the patients show mutations in *Mutl-homolog 1* or *MutS-homolog 2* genes, and is the most frequent inherited CRC syndrome [44]. By contrast, FAP patients develop several (>100) colonic adenomatous polyps, which entails a 100 % risk of CRC at an average age of 40 if no preventive colectomy is performed [1]. FAP is caused by a germline mutation in the *APC* gene, which leads to over activation of Wnt signaling [45].

Recently, a new classification system for CRC has been suggested based on the global gene expression patterns of the tumors [46]. This system subdivides CRCs into four "consensus molecular subtypes (CMS)": CMS1 (14 %) CRCs are thought to be driven by microsatellite instability and *BRAF* mutations, CMS2 (37 %) cancers show activating mutations in the Wnt- and Myc-signaling pathways, CMS3 (13 %) are associated with *KRAS* mutations and metabolic maladjustments, while CMS4 (23 %) tumors depict stromal invasion together with increased angiogenesis, probably due to a dysregulation of TGFβ. CRCs of the CMS4 group show the worst overall five-year survival after diagnosis.

2.4.4 Histopathology

The majority (>90 %) of CRCs are adenocarcinomas originating from the epithelial cells of the colorectal mucosa [44]. By definition, human colorectal adenocarcinomas invade the *muscularis mucosae* into the submucosa [47]. Most colorectal adenocarcinomas are gland forming. This feature is used as the basis of the histopathologic grading, distinguishing between well- (>95 % gland forming), moderately- (50-95 % gland forming) and poorly- (<50 % gland forming) differentiated tumors, although grading systems vary among different clinical centers [44]. For murine colorectal

tumors, the term “intramucosal adenocarcinoma” has been suggested to describe tumors invading through the *lamina propria* into the *muscularis mucosae*, but not reaching the submucosa [48].

2.5 The tumor stroma

The stroma undergoes significant morphological changes during tumor development and progression [7]. The main phenotype of tumor-associated stromal cells is frequently referred to as “cancer-associated fibroblasts” (CAFs), large spindle-shaped cells that comprise a heterogenic group of cells, which are present in nearly all solid tumors [49]. CRCs are characterized by a relatively high abundance of CAFs [50,51] like, for example, breast, prostate and pancreatic cancers [52], while CAFs are sparse in brain, renal, and ovarian cancers. To date, it has not been possible to molecularly define CAFs with specific markers, which highlights their heterogeneity [12]. Two main markers used to identify CAFs are α-SMA and fibroblast-activation protein α (FAPα), but both also mark other cell types and, contrarily, not all CAFs are marked by either α-Sma or FAPα [12]. The heterogeneity of CAFs makes it challenging to identify their origin (Figure 2). The major cells that give rise to CAFs are thought to be resident tissue fibroblasts and MSCs, but an abundance of other cell types may contribute [12].

Among the most important cancer cell-derived factors for the transformation of mesenchymal cells into CAFs is TGF-β, which is also the main driver of the activation of fibroblasts towards myofibroblasts [53], as well as platelet-derived growth factors, basic fibroblast growth factor, and cytokines such as interleukin 6 (IL-6) [12]. Functionally, CAFs are thought to influence tumor development in diverse ways. First, they contribute to changes in the tumor microenvironment, e.g. by the initiation of angiogenesis, the modulation of the tumor metabolism and the immune response. Secondly, CAF-derived factors regulate cancer stemness, promote cancer cell migration and metastasis, and are involved in the alteration of the therapeutic response by remodeling the ECM [12]. Figure 2 illustrates the major characteristics of CAFs.

Data on how the tumor microenvironment in CRC influences cancer development and progression, and how it can be used as a prognostic marker, are sparse and controversial. Most data suggest a pro-carcinogenic role of the tumor stroma: For example, the tumor microenvironment is considered to modulate tumor stemness, i.e. the ability of (undifferentiated) tumor cells to renew themselves, by Wnt pathway alterations [33]. This seems to be in line with the new CMS which describes the CMS4 (mesenchymal) CRCs, defined by high epithelial-to-mesenchymal transition activity, high TGFβ signaling, overexpression of ECM proteins, and high levels of angiogenesis, as the group with the worst overall survival rate [46].

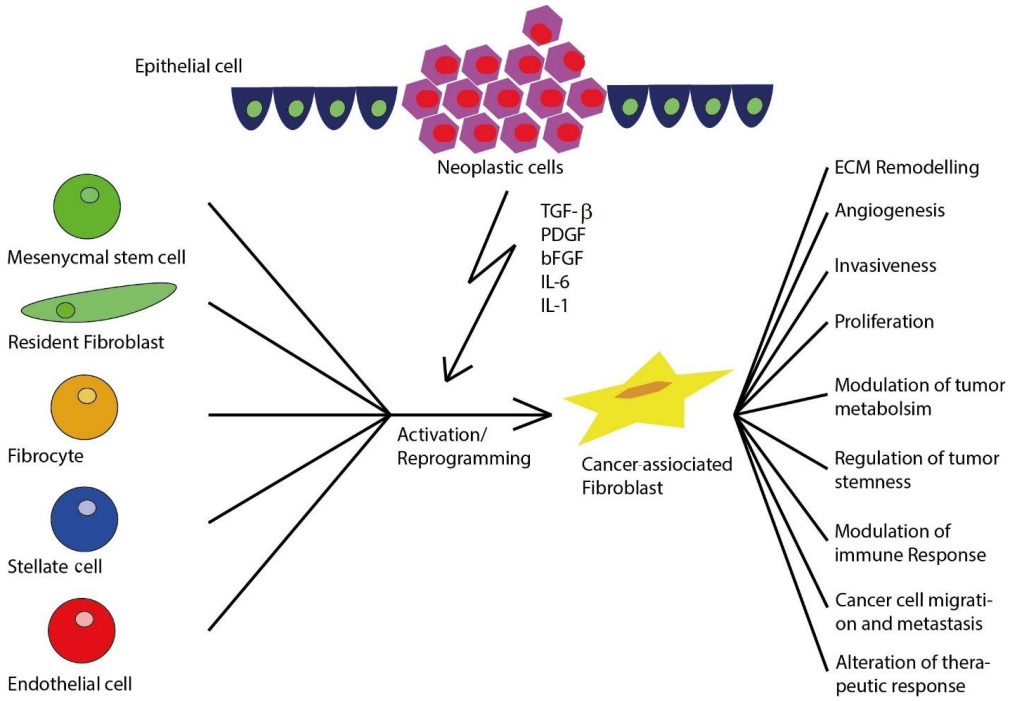

Figure 2. The origin of cancer-associated fibroblasts and their roles in carcinogenesis.

Stromal cells, such as mesenchymal stem cells or resident fibroblasts are reprogrammed by diverse cancer cell-derived factors (e.g. TGF-β, platelet-derived growth factor [PDGF], fibroblast growth factor [FGF]). CAFs play different roles in cancer development as indicated on the right-hand side.

2.6 Hedgehog signaling and cancer

In the majority of human tumors, mutations in Hh-related genes are rare [54]. However, specific cancer types, such as basal cell carcinoma, medulloblastoma, and rhabdomyosarcoma are driven by activating mutations in the Hh pathway [55]. In these tumors, Hh acts as a cell-autonomous driver of tumorigenesis and downstream signaling is activated, most frequently by deactivating mutations in the inhibitory receptor *PTCH1* [55]. This discovery led to the development of Vismodegib, a small-molecule inhibitor of SMO, which lies directly downstream of PTCH1 in the signaling cascade. Vismodegib is the first approved Hh inhibitor for the treatment of advanced basal cell carcinomas [56].

In CRC, expression of the ligand Sonic hedgehog is up-regulated [57]. Moreover, some colon cancer cell lines depend on active Hh signaling for proliferation [58]. These and other data implied hope for a benefit of Hh inhibition with Vismodegib for CRC patients. However, a clinical trial, in which Vismodegib was used as an add-on to conventional chemotherapy in patients with metastatic CRC, did not demonstrate a positive effect, but rather indicated a trend of lower survival in one study arm receiving the Hh antagonist [59]. The authors of the trial discussed several possibilities as to

why the study failed, such as that potential up-regulation of Hh signaling is not the cause for metastatic CRC, or that Vismodegib might interact with the co-therapy [59].

Another tumor type in which Hh signaling was thought to promote carcinogenesis is pancreatic ductal adenocarcinoma (PDAC), which resembles the Hh expression pattern of CRC with an up-regulation of ligand expression. Similarly to CRC, a clinical study with a different SMO inhibitor in patients with PDAC was conducted, which was stopped at interim analysis due to inferior outcome in the group that received the inhibitor (http://www.infi.com/ [homepage on the Internet]. Infinity Pharmaceuticals, Inc.; [updated Jan. 27, 2012; last accessed 20 June 2016]. URL: http://phx.corporate-ir.net/phoenix.zhtml?c=121941&p=irol-newsArticle_print&ID=1653550&highlight=).

Recent data provided insight into potential reasons why Hh pathway inhibition in clinic trials lacks positive effects: PDAC mouse models treated with IPI-926, another specific SMO inhibitor, showed positive effects after a short-term treatment [60], while ongoing inhibition led to decreased survival and higher tumor aggressiveness [61]. Highlighting the role of Hh in the stroma-tumor interaction, deletion of *Shh* in a PDAC mouse model led to diminished stroma, but also to more aggressive tumors with undifferentiated histology and a higher proliferation rate [61]. Recent results point at a potentially protective effect of Hh activation on PDAC: whereas the genetic and pharmacologic inhibition of the Hh pathway results in faster growth of pancreatic neoplasia, pathway activation leads to a decrease in proliferation of mutagenic cells [62].

Complementing the results in PDAC and CRC, a recent publication on bladder cancer provided evidence that the Hh pathway has a protective role in tumor progression, partly mediated by stromal BMPs [63].

Taken together, these results question the paradigm of Hh-driven tumor-promoting stroma and pose the question of how stromal Hh activation influences CRC development and progression.

2.7 Mice in (cancer) research

2.7.1 Colorectal cancer mouse models

Knowledge of the importance of the Wnt pathway in CRC has been applied to create mouse models of intestinal cancer. The Apc^{Min} (Min: multiple intestinal neoplasia) mouse model shows intestinal adenoma formation upon a T-to-A transversion in the mouse *Apc* gene [64], which is largely

restricted to the small intestine [65]. By contrast, tumors in the colon can be induced with chemical carcinogens such as a combination of azoxymethane (AOM) and dextran sodium sulfate (DSS) [66]. AOM is a carcinogen which induces base mispairings by alkylation of DNA and is activated hepatically through a cytochrome P450 dependent process [66]. AOM administration leads mainly to tumors in the distal part of the colon, corresponding to the most common localization of sporadic CRCs in humans [66]. Furthermore, tumors occasionally show invasion through the *muscularis mucosae* [67]. Also on a molecular level, oncogenic pathways show similarities to human CRC, such as up-regulation of Wnt signaling [66]. DSS can be used to accelerate tumor development. DSS is a pro-inflammatory substance, consisting of a complex glucose polymer. It is administered dissolved in the drinking water, consequently harming the epithelium of the murine colon from the luminal side and leading to colitis-associated tumors, while the exclusive administration of AOM can be regarded as a model for sporadic CRC [66].

2.7.2 Genetically modified mice with reporter genes

A reporter gene is an artificially introduced gene used as a readout for the expression of the original gene of interest [68]. The reporter gene, e.g. the enzyme β galactosidase encoded by the bacterial gene *LacZ* (beta-galactosidase lactose Z), can be integrated into a mammalian gene sequence directly downstream of the target gene promoter; cells expressing the gene of interest then also express *LacZ* [69]. Using the enzymatic activity of β - galactosidase by exploiting the enzymatic reaction of its substrate *o*-Nitrophenyl- β -D-galactopyranosid into a blue-colored dye serves as a readout for transcription of the gene of interest [68]. In the case of this study, the Hh downstream transcription factor *Gli1* served as a target gene, resulting in mice with one wild type (wt) *Gli1* allele and one *LacZ* allele (*Gli1*$^{+/lacZ}$ mice) [69] (Figure 3a).

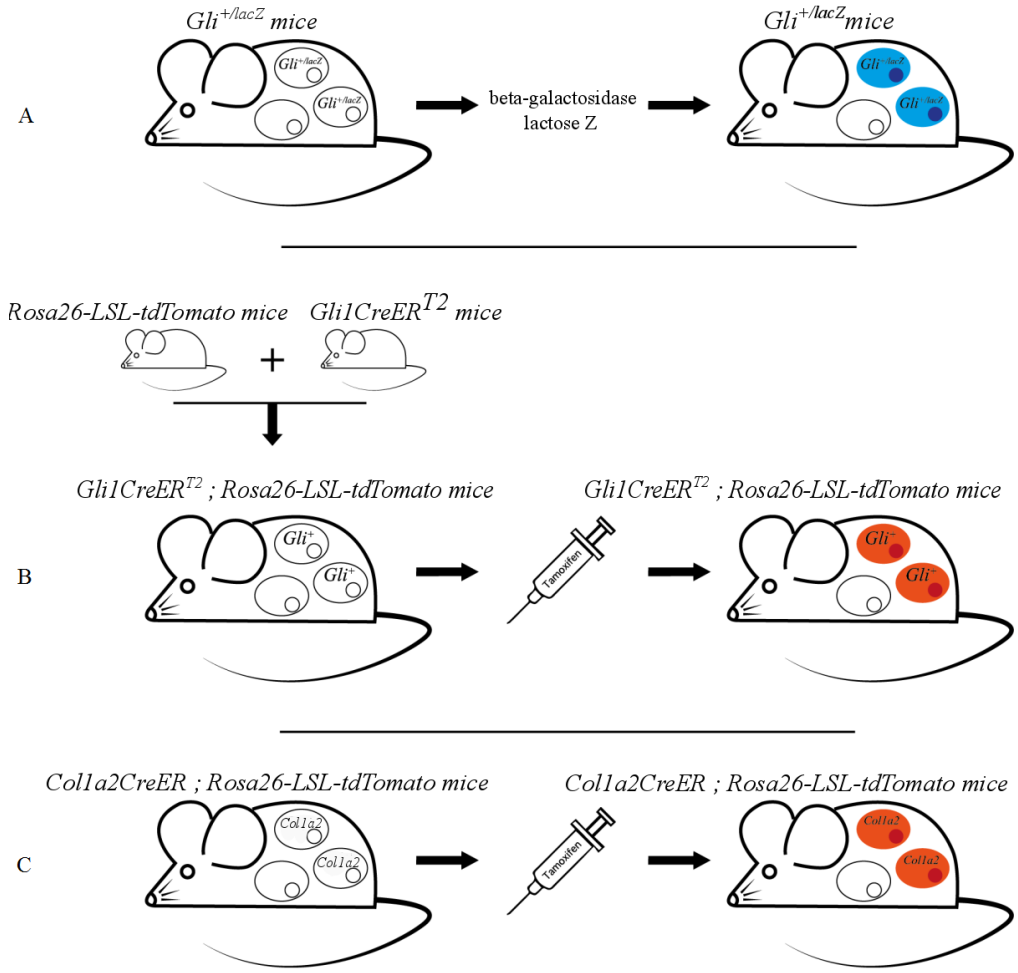

Figure 3. Reporter mice.

(a) In *Gli1*$^{+/lacZ}$ mice the enzymatic activity of beta-galactosidase is used to visualize *Gli1* expressing cells. (b) Crossing *Rosa26-LSL-tdTomato* reporter mice with *Gli1CreER*^{T2} mice (*Gli1CreER*^{T2}*;Rosa26-LSL-tdTomato)* allows visualization of *Gli1* expressing cells after tamoxifen induction. (c) *Col1a2CreER;R26-LSL-tdTomato* reporter mice allow visualization of Collagen1a2 (*Col1a2)* expressing cells after tamoxifen administration.

2.7.3 Cre-Lox recombination in mice

The *Cre-LoxP* system is based on the ability of the enzyme cyclic recombinase (Cre) to delete and invert selected DNA sequences. Cre, as a site-specific recombinase, recognizes a specific sequence (a 34 base pair recombination target site called "Locus of Crossover in P1" [*LoxP*]), which can be flanked around a gene of interest (then referred to as a "floxed" gene). Cre binds to the first and last 13 base pair of the *LoxP* sequence and catalyzes recombination. When the two *LoxP*-sequences follow the same direction, the embedded DNA is cut out and the resulting circular DNA-fragment will be abolished. To invert parts of DNA, antidromic *LoxP* sides are used [70]. To induce recombination in adult mice, Cre-proteins with tamoxifen-inducible domains are available (then called CreERT) [71].

In order to alter Hh activity, for example to achieve Hh activation, *loxP* sites can be flanked around both *Ptch1* alleles [72], while the Cre-recombinase is expressed under a fibroblast-specific promoter, Collagen1a2 (*Col1a2*) [73]. In *Col1a2CreER;Ptch1*$^{fl/+}$ and *Col1a2CreER;Ptch1*$^{fl/fl}$ mice, tamoxifen administration results in *Ptch1* knockout mice exclusively in *Col1a2* expressing cells, either in a single allele (*Ptch1*$^{fl/+}$) or homozygous (*Ptch1*$^{fl/fl}$) (Figure 4). Recombination can be verified indirectly by using a fluorescent protein (e.g. tandem dimer [td]Tomato at the ubiquitous *Rosa26* locus in mice) [74] with a floxed STOP cassette in front as a reporter allele (Figure 3b&c).

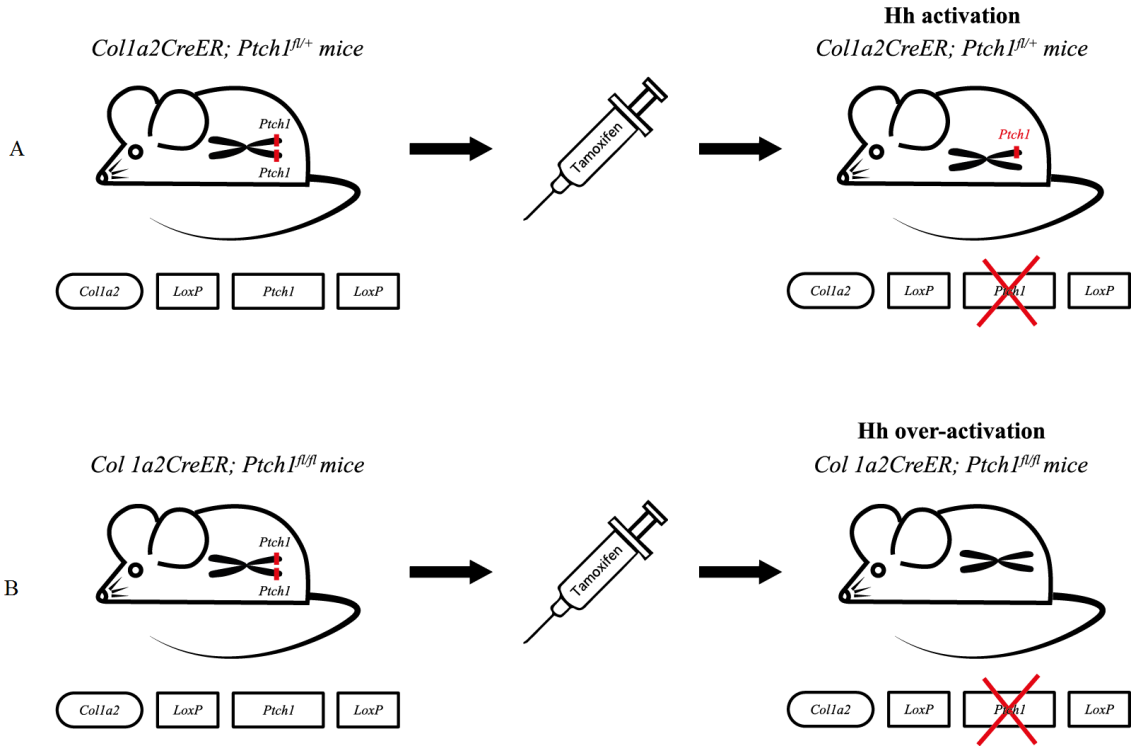

Figure 4. Hedgehog activation in mice via the cyclic recombinase-locus of crossover in P1 recombination.
To achieve Hh activation *loxP* sites are flanked around both *Ptch1* alleles while the Cre-recombinase is expressed under *Col1a2*. In *Col1a2CreER;Ptch1*$^{fl/+}$ (a) and *Col1a2CreER;Ptch1*$^{fl/fl}$ (b) mice, tamoxifen administration results in *Ptch1* knockout exclusively in *Col1a2* expressing cells, either of a single allele (*Ptch1*$^{fl/+}$) or homozygously (*Ptch1*$^{fl/fl}$).

3 Research Aims

Previous studies suggested that the Hh pathway has a tumor-promoting role in CRC, but a clinical trial using a pathway inhibitor yielded a negative result. Therefore, the primary aim of this study was to investigate the role of Hh for development and progression of CRCs using mouse models.

3.1 Hedgehog activity in murine colorectal tumors

While under homeostatic conditions, Hh signals in a paracrine manner in the intestine, it is controversial whether the secretion mode in CRC is autocrine [58,75,76] or paracrine [77]. The first aim of this thesis was therefore to explore if canonical Hh signaling is paracrine or autocrine in murine colon tumors.

3.2 Effect of Hedgehog activation on tumor formation

Since the use of a specific Hh inhibitor in CRC patients failed in a clinical trial, and Hh-driven signals induce epithelial differentiation in non-malignant intestine, the second aim of this thesis was to investigate the consequences of Hh activation on tumor development and progression in murine colon tumors. For this purpose, a mouse model of stroma-specific Hh activation based on the *Cre-LoxP* recombination system was analyzed.

3.3 Stromal changes upon Hedgehog activation

Hh signaling is crucial for the homeostasis of the stroma compartment in the adult intestine. The third aim was thus to analyze the cellular changes induced by stromal Hh activation.

3.4 Crosstalk of Hedgehog and bone morphogenetic protein signaling in colorectal cancer

It has been reported that Hh ligands induce synthesis of stromal BMP agonists. The BMP pathway controls cell differentiation in the normal colon as well as in CRC. Hence, the fourth aim of this thesis was to specifically investigate changes in the expression of members of the BMP pathway upon activation of stromal Hh signaling in the mouse model as well as in human CRC.

4 Materials and Methods

4.1 Materials

4.1.1 Equipment

Equipment	**Company**
Affymetrix Mouse Gene ST 2.0 arrays	Santa Clara (California, USA)
Bright field microscope	Leica DMLB, Leica Microsystems (Wetzlar, Germany)
Centrifuges	Eppendorf centrifuge 5417C, Eppendorf AG (Hamburg, Germany) - Mini Centrifuge C-1200, National Labnet Co. (Edison, NJ, USA) - Galaxy Mini, VWR International Ltd. (Lutterworth, UK) - Beckman Coulter Allegra 25 R Centrifuge Vortex : Kebo-Lab Reax 2000. KEBO Inredningar Sverige AB (Bromma, Sweden)
Charge-coupled device camera	Leica DC 300F
LSM710 confocal microscope	Zeiss (Oberkochen, Germany)
Pressure cooker 2100 retriever	Aptum (Southhampton, United Kingdom)
VDI 12-homogenisator	VWR International, Radnor (Pennsylvyania, USA)
Vevo 2100 high-frequency ultrasound system	Visualsonics (Toronto, Canada)
7500 Fast Real-Time PCR system	Applied Biosystem (Foster City, California, USA)

4.1.2 Reagents, Materials, and Kits

Reagents	**Company**
Alexa Fluor dyes	Invitrogen (Carlsbad, California, USA)
Alkaline phosphatase-labelled streptavidin	Dako (Glostrup, Denmark)
Azoxymethane (AOM)	Sigma-Aldrich (Saint-Louis, Missouri, USA)
Avidin	DAB plus reagent kit – Invitrogen
Biotin	DAB plus reagent kit – Invitrogen
Cold fish skin gelatin (CFSG)	Sigma-Aldrich
Corn oil	Sigma-Aldrich
DIVA reagent	Biocare Medical (Concard, California, USA)
Dextran sodium sulfate (DSS)	Tdb consultancy (Uppsala, Sweden)
Eosin stain solution	Sigma-Aldrich

Reagents	**Company**
Ethanol	Kemetyl Absolut Finsprit 99,5%, Kemetyl AB, (Hanninge, Sweden)
Fast Red	Dako
Glutaraldehyde	Grade I, 50% in H_2O, Sigma-Aldrich
Hematoxylin stain solution	Sigma-Aldrich
Hydrogen peroxide	Sigma-Aldrich
Isoflurane	Baxter (Deerfield, Illinois, USA)
Magnesium chloride	MIK 0665, Karolinska Substratenheten
Methanol	Sigma-Aldrich
Mercaptoethanol, >99%	Sigma-Aldrich
Na-Azide	Sigma-Aldrich
N,N,-dimethylformamide	Sigma-Aldrich
Nonidet P-40	BDH Laboratory Supplies (Dubai)
Paraffin	Sigma-Aldrich
Paraformaldehyde	Sigma-Aldrich
Phosphate buffered saline (PBS)	PBS tablets, Medicago
Potassium hexacyanoferrate (II) trihydrate	Sigma-Aldrich
Potassium hexacyanoferrate (III)	Sigma-Aldrich
PCR reagents: Power SYBR® green PCR Master Mix containing AmpliTaq Gold® DNA Polymerase, heat-activated polymerase, SYBR® green I Dye, buffer components, dNTPs, and ROX	Applied Biosystems
RNeasy midi kit, containing: RLT buffer RW1 buffer RPE buffer	Qiagen (Venlo, Netherlands)
Sodium chloride	Sigma-Aldrich
Streptavidine peroxidase	Invitrogen
SuperScript ® III First-Strand Synthesis System containing: RT buffer,	Invitrogen

Reagents	Company
DTT, RNase OUT SuperScript ® III RT oligo deoxythymidylic acid (dT) and desoxynucleosid triphosphate (dNTP) mix	
Tamoxifen	Sigma-Aldrich
Topro-3	Invitrogen
Tween 80 for molecular biology	Sigma-Aldrich
Triton X-100	Sigma-Aldrich
Water based mounting medium	Polyscience (Warrington, Pennsylvania, USA)
X-gal	Sigma-Aldrich
Xylene	Sigma-Aldrich
3,3´-Diaminobenzidine (DAB)	DAB plus reagent kit – Invitrogen
4OH-Tamoxifen	Sigma-Aldrich
5-Bromo-4-chloro-3-indolyl-beta-D-galactopyranoside	Sigma-Aldrich

4.1.3 Solutions

Solution	Concentration
X-gal substrate solution	stock solution: 100 ml washing buffer, 1 ml 5 mM potassium ferricyanide, 1 ml 5 mM potassium ferrocyanide, and 2.5 ml 40 mg/ml 5-bromo-4-chloro-3-indolyl-beta-D-galactopyranoside in N,N,-dimethylformamide
Immunofluorescence blocking solution	5 % BSA in PBS/Tx-100 + 0.01 % Tween
Immunohistochemistry blocking solution	5% Serum in 1% BSA/PBS, 0.2% CFSG, 0.1% Tx-100, 0.1% Na-Azide

4.1.4 Databases and Software

Databases/software/plugins	**Source**
AmiGO2 database v 2.1.4	https://www.geneontology.org (last accessed 2017-04-01)
Gene expression omnibus (GEO)	https://www.ncbi.nlm.nih.gov/geo (last accessed 2017-04-01)
GraphPad Prism 6.0e software	https://www.graphpad.com/, La Jolla, California (last accessed 2017-04-01)
GSEA Java plug-in v2.1.0	https://www.software.broadinstitute.org/gsea/index.jsp (last accessed 2017-04-01)
ImageJ´s color deconvolution plug-in	https://imagej.nih.gov/ij/[homepage on the Internet]. ImageJ; color deconvolution plug-in; (last accessed 2017-04-01). URL: http://www.mecourse.com/landinig/software/cdeconv/cdeconv.html
Molecular signature data base (MSigDB)	www.broadinstitute.org/gsea/msigdb, Broadinstitut, Cambridge, United Kingdom (last accessed 2017-04-01)

4.2 Mice

R26-LSL-tdTomato (*B6.Cg-Gt[ROSA]26Sortm14[CAG-tdTomato]Hze/J*) mice were purchased from The Jackson Laboratory (Bar Harbor, ME; Farmington, CT; and Sacramento, CA; all USA); *Col1a2CreER* (*B6.Cg-Tg[Col1a2-cre/ERT]7Cpd/J*) mice were imported from Benoit de Crombrugghe's laboratory (Houston, Texas, USA); $Gli1^{lacZ/+}$ ($Gli1^{tm2Alj}/J$) and $GliCreER^{T2}$ mice ($Gli1^{tm3(cre/ERT2)Alj}/J$) were obtained via the Fritz Aberger laboratory (Salzburg, Austria) and originally developed in Alexandra Joyner's laboratory (see Table 2). C57BL/6J mice were bought from Scanbur (Sweden). $Ptch1^{fl/+}$ mice were developed in the host laboratory and described earlier [72]. All backcrossings were to C57BL/6J mice. Mice were housed as littermates, separated according to sex. In the case of genetically modified *Cre-LoxP* mice, littermate controls did not bear the *Cre* allele, the floxed alleles or both and were otherwise treated similarly to *Cre-LoxP mice*.

Ethical approval for animal experiments was obtained from the local ethics committee (permits S69/12, S138/12, S10/15, S15/15, and extensions, *Jordbruksverket*, Sweden).

We monitored the health status of the mice according to the Karolinska Institute's scale for the assessment of laboratory animals (in a cumulative score including skin condition, movements and body posture, piloerection, breathing, excretions, ocular so-called porphyrin production, and food uptake). Mice on DSS were weighed daily and euthanized according to ethical guidelines.

Mice	Characteristics	Reference
Gli1$^{lacZ/+}$	Reports *Gli1* expression as robust readout of active downstream Hh signaling.	Bai *et al.* [69]
Gli1CreER^{T2}	Inducible, Cre-driven recombination in cells with active downstream Hh signaling (stromal cells in case of the intestine)	Ahn and Joyner [78]
Col1a2CreER	Inducible, fibroblast specific transgenic Cre-driver (targeting a cell population overlapping partly with *Gli1*$^{+}$ cells)	Zheng *et al.* [73]
Ptch1$^{fl/+}$	Inducible knockout of one *Ptch1* allele to activate Hh signaling in the targeted cells capable of Hh signaling transduction.	Kasper *et al.* [72]
Ptch1$^{fl/fl}$	Homozygous variant of the above; function as in *Ptch1*$^{fl/+}$, but stronger activation of Hh signaling can be expected.	Kasper *et al.* [72]
R26-LSL-tdTomato	Reporter mice expressing the fluorescent protein tandem dimer [td]Tomato downstream of a floxed STOP cassette	Madisen *et al.* [74]

Table 2. Mice genotypes and their specific characteristics as used in this thesis. (Hh = Hedgehog, Gli = glioma-associated protein homologue, Cre = cyclic recombinase, Ptch = Patched, Col1a2 = Collagen1a2)

4.3 Chemical models of colorectal cancer

Colonic tumors were induced by giving the mutagenic agent AOM at 12.5 mg/kg body weight intraperitoneally (day 0), followed by administration of a 2 % w/v DSS drinking solution for 5 days starting on day 5 (Figure 5a). Two further DSS cycles were given, interrupted by two weeks of regular drinking water. Alternatively, AOM was administered weekly (12.5 mg/kg body weight) for ten consecutive weeks, without addition of DSS (Figure 5b).

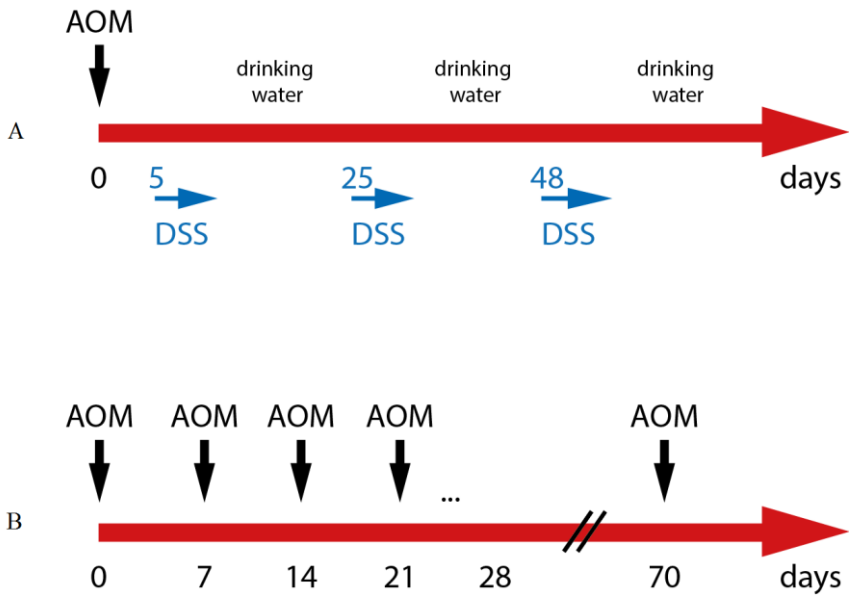

Figure 5. Schematic of azoxymethane/dextran sodium sulfate and azoxymethane treatments.
(a) AOM/DSS model. Mice received AOM intraperitoneally (day 0), before DSS was given (day 5) orally for 3 cycles, with normal drinking water for two weeks in between. (b) AOM model. AOM was given weekly for ten consecutive weeks. (AOM = azoxymethane, DSS = dextran sodium sulfate)

4.4 Tamoxifen treatment

Mice received 1 mg 4OH-Tamoxifen (diluted in ethanol and corn oil) per 25 g bodyweight intrarectally using a plastic gavage tube to limit extracolonic recombination [79].

In the case of *Col1a2CreER or Gli1CreER^{T2};R26-LSL-Tomato* labeling studies, 5 mg tamoxifen was injected intraperitoneally at 20 mg/ml, dissolved in corn oil.

4.5 High-frequency ultrasound

For quantification of tumor number and size, the Vevo 2100 system high-frequency ultrasound system was used, based on a method described previously [80]. Briefly, mice were scanned with a 40 MHz US probe from the rectum rostrally while under anesthesia. The largest tumor diameter was identified visually and the tumor border was drawn manually.

4.6 Immunohistochemistry

4.6.1 Avidin-biotin complex method

The avidin-biotin complex method is a routine technique for immunohistochemical (IHC) staining based on the high affinity of avidin, a glycoprotein, and strepatavidin (*Streptomyces avidinii*) to

the vitamin biotin. The biotinylated secondary antibody acts as a link between the region of interest (antigen), the primary antibody, and an avidin-biotin-peroxidase complex. The peroxidase complex enzymatically synthesizes a colored product, which visualizes the expression of the protein of interest.

4.6.2 3,3´-Diaminobenzidine staining

Four-µm thick paraffin-embedded colon sections were generated by cutting colons longitudinally, before being placed in 4 % paraformaldehyde/phosphate buffered saline (PBS) at 4 °C > 8 h for fixation. After a 1 h baking step (60 °C) and rehydration, a heat-induced epitope retrieval step with DIVA reagent was performed using a pressure cooker. After blocking of endogenous peroxidase activity by hydrogen peroxide (3 %), the sections were incubated with diluted primary antibody (Table 3) for 1 h (room temperature [RT]) in a moist chamber. Negative controls were performed by omitting the primary antibody. The rinsed sections were incubated with biotinylated secondary antibody (Table 3; 1:200) for 30 min in the same manner, before streptavidin peroxidase or alkaline phosphatase-labelled streptavidin (only β-catenin) administration for 30 min at room temperature. For visualization, peroxidase-treated sections were incubated with 3,3´-Diaminobenzidine (DAB) or alkaline phosphatase with Fast Red; counterstaining was performed by using hematoxylin or eosin (for X-gal stained tissue). Sections were mounted with water-based mounting medium.

Primary Antibody	Dilution	Secondary Antibody
β-catenin (Cell Signaling, Danvers, Massachusetts, USA; #9582)	1:100	Goat anti-rabbit (Vector [Burlingame, California])
phospho-Smad1/5 (Ser463/465; Cell Signaling; 9516S)	1:50	Goat anti-rabbit (Vector)
Desmin (Abcam, Cambridge, United Kingdom, ab8592)	1:200 (IF:1:500)	Goat anti-rabbit (Vector)
Vimentin (Santa Cruz, Dallas, Texas, USA C20)	1:200 (IF: 1:500)	Rabbit anti-goat (Vector)
α-Sma (Abcam, ab5694)	1:200 (IF: 1:500)	Goat anti-rabbit (Vector)
anti-collagen1(Abcam, ab34710)	IF: 1:200	Goat anti-rabbit (Vector)
Prox1 (R&D Systems, Minneapolis, USA, #AF2727)	1:200	Rabbit anti-goat (Vector)

Table 3. Primary antibodies, dilutions, and complementary secondary antibodies.

4.6.3 X-gal staining

The staining was done according to Kasper *et al.* with slight modifications [72]. After fixation in 2 % PFA/PBS with 0.2 % v/v glutaraldehyde for 30 min at room temperature, tissues were washed in 2 mM magnesium chloride in PBS plus 0.01 % Nonidet P-40 for 15 min. After a 15 h incubation step at 37 °C in X-gal substrate solution (stock solution: 100 ml washing buffer, 1 ml 5 mM potassium ferricyanide, 1 ml 5 mM potassium ferrocyanide, and 2.5 ml 40 mg/ml 5-bromo-4-chloro-3-indolyl-beta-D-galactopyranoside (X-gal) in N,N,-dimethylformamide), the samples were washed in PBS and fixed in 4 % PFA/PBS for 4 h at RT before paraffin embedding.

4.6.4 Quantification of X-gal and DAB staining

Slides were examined with a standard bright-field microscope and pictures were taken using a charge-coupled device camera. The images were used for quantification of DAB and X-gal intensities with ImageJ´s color deconvolution plug-in with manual definition of the regions of interest. Pixel intensities for DAB (brown) and X-gal (blue) were quantified on an 8-bit scale.

4.6.5 Immunofluorescence

Immunofluorescence (IF) staining was done on frozen sections, cut in 20-100 um thickness. The normal serum blocking solution consisted of 5 % BSA in PBS/0.5% Tx-100. The diluted primary antibody (Table 3) was incubated overnight immediately after a 30-minute blocking step, before washing and incubation of the secondary antibody (in a concentration of 1:250, 45 min, Alexa Fluor dyes). Nuclear staining was performed with TOPRO-3 or DAPI 1:1000 in PBS. The results were examined using a Zeiss LSM 710 confocal microscope.

4.7 Real-time quantitative polymerase chain reaction

Real-time quantitative polymerase chain reaction (RT-qPCR) is an amplification method for nucleoid acids allowing the quantification of DNA.

4.7.1 Purification of ribonucleic acid

RNA was isolated using the RNeasy midi kit, following the manufacturer's instructions. The principle is based on the selective binding of RNA to a silicon-gel membrane, enriching for messenger RNA (mRNA). Twenty -30 mg snap frozen sample was used, either containing tumor tissue or normal colon tissue. Immediately prior to RNA extraction, samples were thawed from -80 °C.

Briefly, the frozen tissues were added into 600 µl "RLT buffer" (kit reagent) plus 6 µl mercaptoethanol and homogenized using a VDI 12-homogenisator. Homogenates were then centrifuged for 3 min at full speed (14000 x *g*) and supernatants were discharged before 600 µl of 70 % ethanol was added to the cleared lysate. Up to 700 µl of the mixture was transferred to an "RNeasy" spin column placed in a 2 ml collection tube and centrifuged for 15 s at 8000 x *g*. The flow through was discarded and the procedure was repeated until no lysate was left. 700 µl of "RW1 buffer" (kit reagent) were added to the RNeasy spin column and centrifuged again with the same settings. 500 µl of "RPE buffer" (kit Reagent) were added to the spin column and the sample was centrifuged first for 15 s at 8000 x *g* and after for 2 min at the same speed.

RNA was subsequently eluted in 30 µl RNA-free water and immediately placed on ice. RNA quality and quantity was assessed photometrically. Ratios between 1.8-2.2 (260/280 nm) were considered pure [81] and concentrations > 500 ng/µl sufficient.

4.7.2 First strand complementary deoxyribonucleic acid synthesis

To synthesize first strand complementary DNA (cDNA) from the purified RNA, the SuperScript ® III First-Strand Synthesis System for RT-PCR was used according to the manufacturer's protocol. Briefly, a cDNA synthesis master mix was prepared. For each sample, 4 µl 5X RT Buffer, 1 µl 0.1 M DTT, 1 µl RNase OUT, and 1 µl SuperScript ® III RT (200 U/µl) were placed in an autoclaved 1.5 ml Eppendorf tube. For negative controls SuperScript ® III RT was replaced by RNase-free water.

Next, 1 µl 50 µM oligo deoxythymidylic acid (dT), 1 µl 10 mM deoxynucleoside triphosphate (dNTP) mix, 1 µg total template RNA, and RNase-free water were incubated in a microcentrifuge tube at 65 °C for 5 min to denature the RNA before being placed on ice for 1 min. The amount of RNase-free water was calculated as shown:

dH_20 = 13 µl (total amount)- 1 µl 10 mM dNTP mix- 1 µl 50 µM oligo(dT) – X µl template RNA (amount of sample containing 1 µg RNA)

Subsequently, 7 µl of the cDNA synthesis master mix was added to each RNA mixture. Finally, the samples were incubated for 50 min at 50 °C to run the cDNA synthesis, and the reactions were terminated by heating to 85 °C for 5 min.

4.7.3 Real-time quantitative polymerase chain reaction

We used a SYBR green-based qPCR method. SYBR green is a fluorescent dye, which binds double-stranded DNA and increases its signal after binding compared to the unbound dye in free solution. The double-strand dye complex absorbs blue light with a wavelength of 488 nm and emits green light (522 nm), which can be detected [82].

As every cycle results in an approximate doubling of the amount of double-stranded DNA in optimal conditions, the fluorescence signal will increase exponentially. Real-time PCR was performed by using a Power SYBR® green PCR Master Mix, consisting of AmpliTaq Gold® DNA Polymerase, heat activated polymerase, SYBR® green I Dye, buffer components, dNTPs, and ROX as passive reference dye. A 7500 Fast Real-Time PCR System was used. Master mixes for target and housekeeping genes were generated by adding 14 µl dH_2O, 19 µl Fast SYBR green MM, and 1µl 1:5 diluted primer mix (Table 4) per sample-triplicate into an autoclaved Eppendorf tube (1.5

ml). The primer dilution consisted of 80 µl RNase-free water and of 10µl forward- and 10µl reverse-Primer; *RPLP0* and *GAPDH* were used as housekeeping genes.

Subsequently, 2 µl template DNA was added to each reaction mix aliquote (10 µl per well). Triplicates were performed as technical repeats. A run consisted of a 10 min heating step and 40 cycles with each 10 s for denaturation at 95 °C and 30 s at the appropriate annealing temperature for annealing and elongation. The delta C_T method served to calculate relative mRNA expression, and compared the ΔC_T values of the samples of interest with control mice samples after normalization to the housekeeping genes [83].

First, we calculated the ΔC_T (C_T(target)-C_T(housekeeping)), before the $\Delta\Delta C_T$ (ΔC_T (sample of interest)-ΔC_T (control mice)) was calculated to quantify the relative change in expression between two samples (e.g. non-tumor to tumor tissue). Finally, $\Delta\Delta C_T$ was converted into the n-fold expression: $n\text{-}fold = 2^{-\Delta\Delta Ct}$.

Gene product	**Full Name**	**Sequence**
Gapdh	Glyceraldehyde-3-phosphate dehydrogenase	forward: GGTGTGAACGGATTTGGCCGTATTG reverse: CGTTGAATTTGCCGTGAGTGGAGT
Rplp0/ARP	Ribosomal protein, large, P0/ acidic ribosomal protein	forward: GCACTCTCGCTTTCTGGAGGGTGT reverse: ATGCAGATGGATCAGCCAGGAAGG
Gli1	GLI family zinc finger 1	forward: CGTTTAGCAATGCCAGTGACC reverse: GAGCGAGCTGGGATCTGTGTAG
Ihh	Indian hedgehog	forward: GGCTTCGACTGGGTGTATTA reverse: CGGTCCAGGAAAATAAGCAC
Ptch1	Patched 1	forward: TTGGGATCAAGCTGAGTGCTG, reverse: CGAGCATAGCCCTGTGGTTCT
Shh	Sonic hedgehog	forward: TGGAAGCAGGTTTCGACTGG reverse: GGAAGGTGAGGAAGTCGCTGT
Gli2	GLI family zinc finger 2	forward: TGAGGAGAGTGTGGAGGCCAGTAGCA reverse: CCGGGGCTGGACTGACAAAGC
Hhip	Hedgehog-interacting protein	forward: TAACGGCCCTTTGGTTGGTGGATTT reverse: AGCAAAGCCCAGTGACCAAGCAATG
Grem1	Gremlin 1	forward: AGACCTGGAGACCCAGAGTA reverse: GTGTATGCGGTGCGATTCAT
Nog	Noggin	forward: AAGGATCTGAACGAGACGCT reverse: GCGAAGTAGCCATAAAGCCC

Gene product	Full Name	Sequence
Chrdl	Chordin-like	forward: GATGCTGTTCCCACTGCAC reverse: GGCCCATCCTCTTGGTCATA
Bambi	BMP and activin membrane-bound inhibitor homolog	forward: CGCCACTCCAGCTACTTCTT reverse: TGAGCAGCATCACAGTAGCA
Lgr5	Leucine-rich repeat-containing G protein-coupled receptor 5	forward: CCAATGGAATAAAGACGACGGCAACA reverse: GGGCCTTCAGGTCTTCCTCAAAGTCA
Axin2	Axin 2	forward: CAGGAGGATGCTGAAGGCTCAAAGC reverse: CTCAAAAACTGCTCCGCAGGCAAAT

Table 4. Primers for quantitative polymerase chain reduction. (Gli = Glioma-associated protein homologue, BMP = Bone morphogenetic protein)

4.8 Microarrays

Gene expression microarray analyses allow us to profile gene expression of many different genes at the same time and have become a common tool in research [84,85]. For microarrays, RNA was extracted as described above. Gene expression profiling with RNA of *Col1a2CreER;Ptch1*$^{fl/fl}$ mice and controls was performed using Affymetrix Mouse Gene ST 2.0 arrays in collaboration with the Bioinformatics and Expression Analysis core facility at the Karolinska Institute. To assess differential expression of preselected gene sets representing defined signaling pathways, we applied gene set enrichment analysis (GSEA) [85], using the GSEA Java plug-in v2.1.0 to test non-log-transformed normalized expression data with standard settings (exceptions: the permutation modus was set to "gene_set", and gene sets <15 genes were accepted). The gene list for BMP inhibitors was generated using the AmiGO2 database v 2.1.4 and the list for Hh signaling was retrieved from the molecular signature database (MSigDB).

4.9 Analysis of Gene Expression Omnibus data sets

Gene Expression Omnibus (GEO) is an online database of the US National Center for Biotechnology Information which collects data of gene expression analysis [86]. We analyzed two different data sets derived from mesenchymal cells treated with Hh ligands *in vitro* (GSE17840 and GSE29316) [25,87]. The data were accessed using the GEO website. The microarray data were normalized with the robust multi-array average (RMA) algorithm using the "affy" package for R [88] and differential expression between treatment groups was analyzed using limma [89]. We selected genes of interest (associated to Hh and BMP pathways) and compared differential expression in

Hh ligand treated cells compared with vehicle-treated controls. The false discovery rate (Benjamini-Hochberg), fdr, was set to <0.05 [90].

4.10 Statistical analyses

Data analyses (except for microarray and GEO data) were performed using GraphPad Prism 6.0e software. Data is presented as the mean and standard error of the means (SEM) unless otherwise specified. To compare normally distributed data in two samples, the Student's t-test was used. The type 1-error rate was set to 5 % (*≤ 0.05; **≤ 0.01; ***≤ 0.001). Further specific statistical tests are indicated in the text or in the respective figure legends. Bioinformatic programming and analyses were performed by Simon Joost, Maria Kaspers group, at Karolinska Institutet.

5 Results

5.1 Locally advanced tumors upon AOM/DSS treatment

Many models of intestinal tumors, such as the *Apc*^{min} model, are limited to early tumor stages. For the AOM/DSS model, invasiveness has been reported, while this feature showed dependence on the mouse strain used [91]. The earliest invasive tumor, often referred to as "intramucosal adenocarcinoma" *per definitionem* invades into the *lamina propria* [48]. In our case, mice treated with AOM/DSS occasionally developed adenocarcinomas that invaded the *muscularis mucosae*. Figure 6 provides representative images of invasive tumors [79]. In the example presented in Figure 6a, the *muscularis mucosae* is discontinuous, with tumors cells appearing to break through; and in the tumor in Figure 6b, neoplastic cells are found below the *muscularis mucosae*, in parallel to tumor-induced changes in the stroma (desmoplasia), as an indirect sign of invasiveness. Yet, due to the difficulties to distinguish histologically between invasion and mucosal herniation, which is very frequent in mice [67], we did not further quantify invasiveness. Distant metastases were not seen on gross macroscopic inspection of the abdominal cavity and the liver.

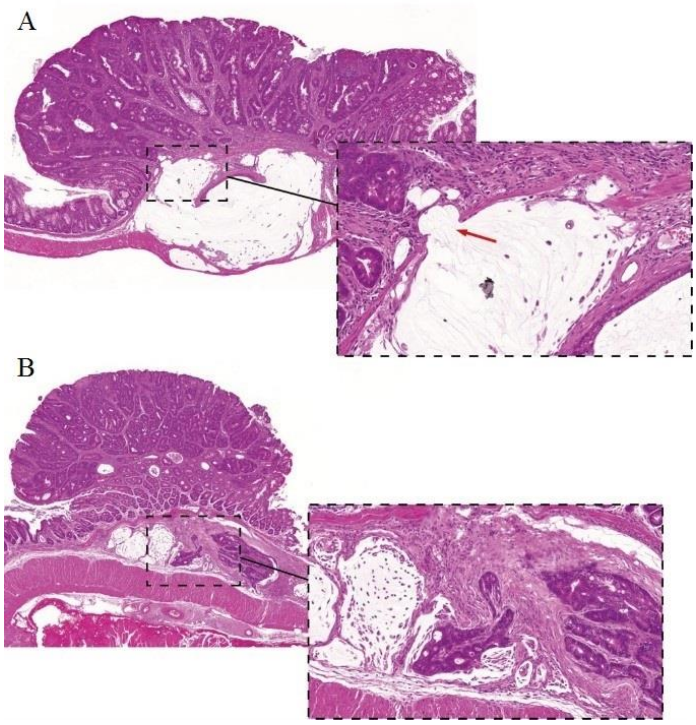

Figure 6. Histology of invasive AOM/DSS-induced carcinoma, hematoxylin/eosin stained colon sections.
(a) Invasive tumor. Arrow indicates interrupted *muscularis mucosae*. (b) Invasive tumor with malignant cells below the *muscularis mucosae*, mucus lakes and desmoplastic stromal reaction (magnification) [79].

5.2 Decreased Hedgehog signaling in AOM/DSS-derived colon tumors

AOM/DSS-induced tumors of *Gli1*$^{lacZ/+}$ mice were used to analyze Hh pathway activity in colonic tumors, since the lacZ reporter indicates *Gli1* transcribing cells that define activated downstream Hh signaling. Both macroscopic (Figure 7) and microscopic stainings (Figure 8a&b) indicated weaker X-gal-staining in the tumors compared to the adjacent mucosa.

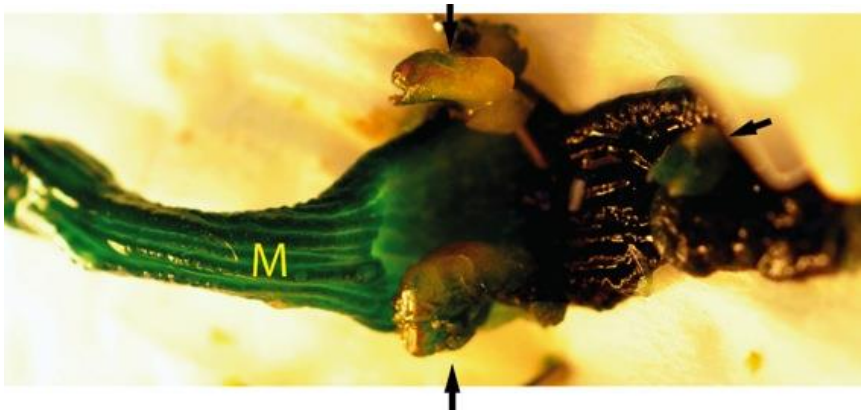

Figure 7. Macroscopic appearance of *Gli1*$^{lacZ/+}$ X-gal stained tumors.

Gli1$^{lacZ/+}$ mice report downstream Hh expression. Non-malignant mucosa (M) showed strong X-gal staining (turquoise) while the tumors (arrows) showed reduced staining. Representative image of n > 20 tumors from n = 11 mice.

5.3 Hedgehog activity remains stromal and is decreased in tumors

Histological analysis of whole-mount X-gal stained tissue from *Gli1*$^{lacZ/+}$ mice with AOM/DSS-induced tumors did not reveal epithelial X-gal staining, neither in normal mucosa (Figure 8a), nor in tumors (Figure 8b). In both tumors and normal mucosa, Gli1 expression, as visualized by X-gal staining, was limited to the stroma (Figure 8). In addition, we found that the tumors showed a weaker lacZ signal compared to the adjacent mucosa (Figure 8b), since blue cells appeared largely absent in the tumor center [79].

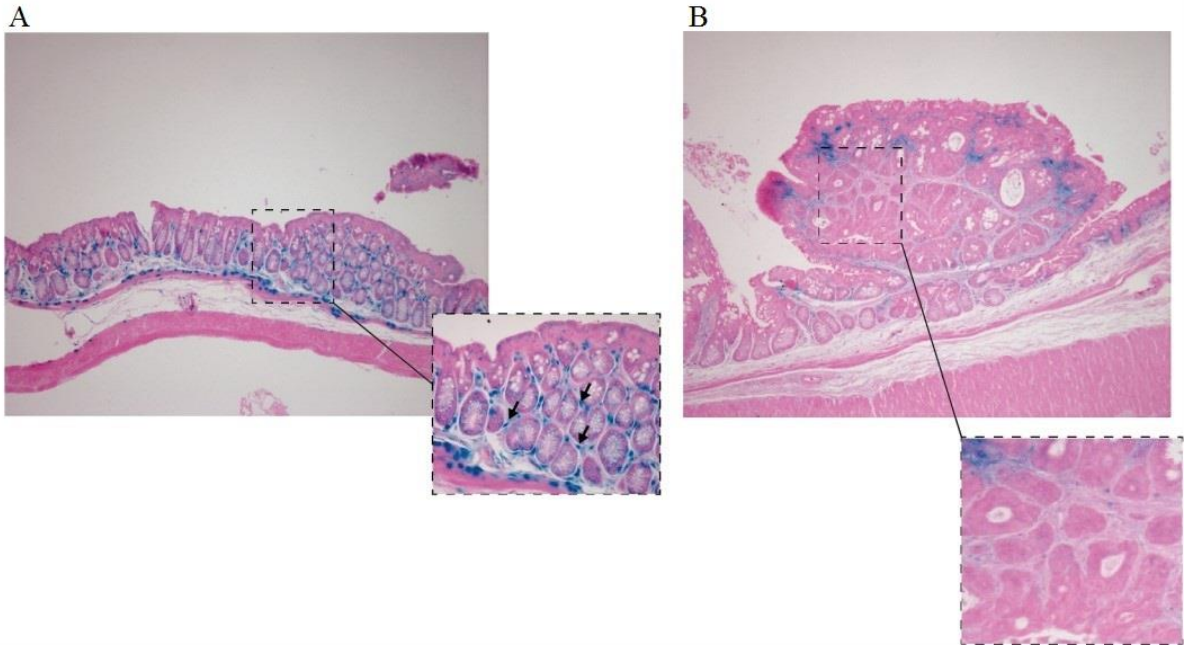

Figure 8. Microscopic appearance of *Gli1*$^{lacZ/+}$ X-gal stained colon tissue after azoxymethane/dextran sodium sulfate treatment.

Normal mucosa and an AOM/DSS-induced tumor using X-gal staining to visualize Gli1 expression (a) normal mucosa, arrows point at positive X-gal stained cells (blue), which are located in the stroma. (b) AOM/DSS-induced tumor with a reduction of X-gal stained cells in the tumor center [79].

5.4 Decreased Hedgehog signaling is paralleled with increased expression of Wnt targets

To confirm the Hh expression patterns in AOM/DSS-induced tumors on the mRNA level, we used RT-qPCR to quantify mRNAs in AOM/DSS-induced tumors and non-malignant mucosa. We found that *Gli1*, *Gli2*, and *Hhip* expression, representing Hh target genes, was significantly reduced in tumors (Figure 9a, b&c). The mRNA levels of *Ptch1* and *Ihh* (Figure 9f&g) in tumors were not significantly different to those in normal mucosa. By contrast, we found the expression of canonical targets of Wnt signaling, *Lgr5* and *Axin2*, significantly increased in tumors (Figure 9d&e) [79].

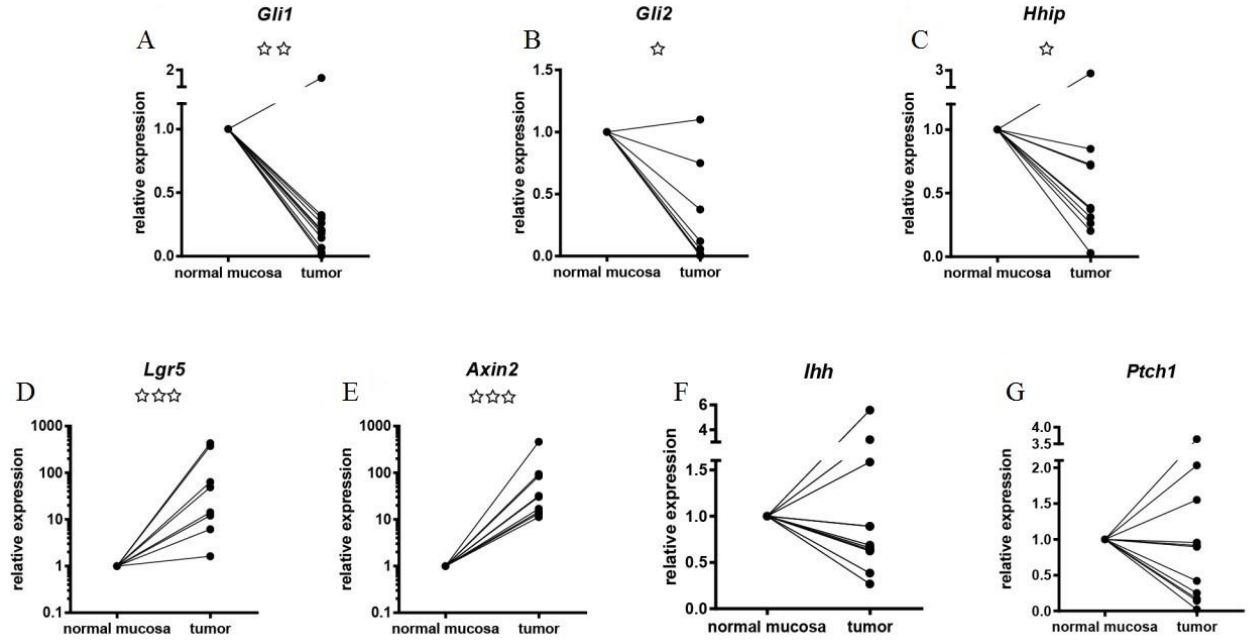

Figure 9. RT-qPCR for Hedgehog and Wnt pathway signals of tumors and matched mucosa.

Comparison of mRNA expression of Hh (*Gli1*, *Hhip*, *Ptch1*, *Ihh*) and Wnt (*Lgr5*, *Axin2*) pathway members in normal mucosa compared to that in tumors relative to the housekeeping gene. Hh signals: (a) *Gli*; n = 11 (b) *Gli2*; n = 10 (c) *Hhip*; n = 10 (f) *Ihh*; n = 11 (g) *Ptch1*; n = 11. Wnt signals: (d) *Lgr5*; n = 8 (e) Axin2; n = 9

(all paired t-tests based on the ΔCT values, *p ≤ 0.05; **p≤ 0.01; ***p ≤ 0.001; multiple test corrected p-values: Gli1: 0.002; Gli2: 0.019; Hhip: 0.044; Ptch1: 0.170; Ihh: 0,1; Axin2: < 0.0001; Lgr5: 0.001) [79]

5.5 Wnt and Hedgehog pathways are negatively correlated in AOM/DSS tumors

Because Wnt pathway activation leads to accumulation of β-catenin protein in the nucleus, we used IHC against β-catenin as a readout for Wnt activity in tumors of *Gli1*$^{lacZ/+}$ mice (Figure 10a). In areas of high Wnt activity indicated by nuclear translocation of β-catenin, the stromal X-gal signal was reduced, suggesting that Hh signaling is downregulated. Furthermore, we observed that Wnt signaling appears to be more active in the tumor center than in its periphery, while X-gal staining was stronger in the periphery (Figure 10b) [79].

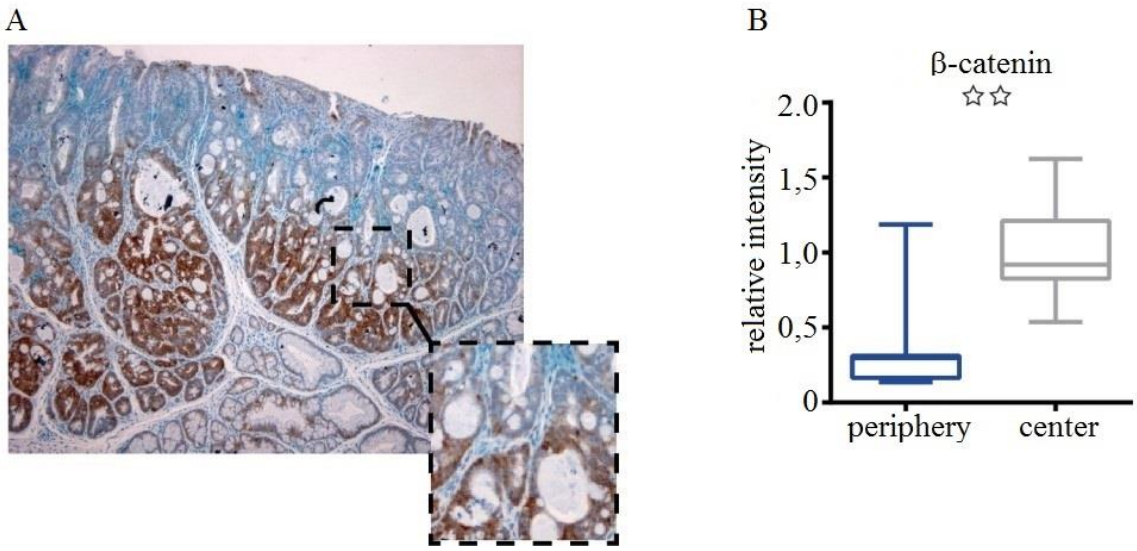

Figure 10. Immunohistochemistry for β-catenin of X-gal-stained tumors in *Gli1*$^{lacZ/+}$ mice.

(a) IHC for ß-catenin in a X-gal-stained *Gli1*$^{lacZ/+}$ tumor, hematoxylin counterstain. Dark blue color indicates positive X-gal staining; light blue is hematoxylin counterstain; brown (DAB) shows ß-catenin expressing cells. (b) Quantification of the difference in intensity between tumor periphery and center in β-catenin stainings, p = 0.0061 (unpaired t-test; **p ≤ 0.01) [79]

5.6 Stromal cells with active Hedgehog signaling

Gli1$^{lacZ/+}$ mice indicated that downstream Hh activity is limited to certain cells in the colon stroma. These results confirmed previous reports that suggested that downstream Hh activation in the intestine is restricted to the stroma [23]. To independently confirm this finding, we generated a different Hh reporter mouse by crossing *Rosa26-LSL-tdTomato* reporter mice with *Gli1CreER*^{T2} mice (*Gli1CreER*^{T2}*;Rosa26-LSL-tdTomato)* (Figure 3). This model allows the visualization of *Gli1* expressing cells after tamoxifen-induced Cre-mediated recombination in thick frozen sections using confocal microscopy [92]. To define the Hh target cells in a near-native environment [92], we combined confocal detection of tdTomato^{+} cells with immunofluorescence against the stromal markers desmin, vimentin, and α-Sma in whole-mount colon samples from *Gli1CreER*^{T2}*;Rosa26-LSL-tdTomato* mice shortly after tamoxifen induction. These analyses confirmed that Gli1 expressing cells are located in the colon stroma and not in the epithelium and indicated that they comprise a mixed cell population, expressing either one of the three markers or a combination of them (Figure 11a,c&e).

For subsequent experiments, we aimed at activating Hh signaling by knocking out *Ptch1* in its downstream target cells. However, in *Gli1CreER*^{T2} mice, *Cre* is knocked into the *Gli1* locus [69], abolishing the function of one *Gli1* allele. As this loss of function of *Gli1* could influence downstream Hh signaling when using *Gli1CreER*^{T2} mice to drive *Ptch1* knockout, we made use of another model, in which *Cre* expression is driven by a transgenic collagen, type I, alpha 2 (*Col1a2*) promoter [73] (Figure 3). IF of *Col1a2CreER;R26-LSL-tdTomato* reporter mice revealed similarities to the *Gli1CreER*^{T2} model, as an overlapping stromal cell population expressing all three stromal markers was targeted by *Col1a2CreER* (Figure 11b, d&f). To confirm that *Col1a2CreER* targets a cell population similar to the *Gli1CreERT2* model, we stained *Gli1CreER*^{T2}*;R26-LSL-dtTomato* mice with IF for collagen 1 protein and observed an overlap of tdTomato and Col1 expression (Figure 11g) [79].

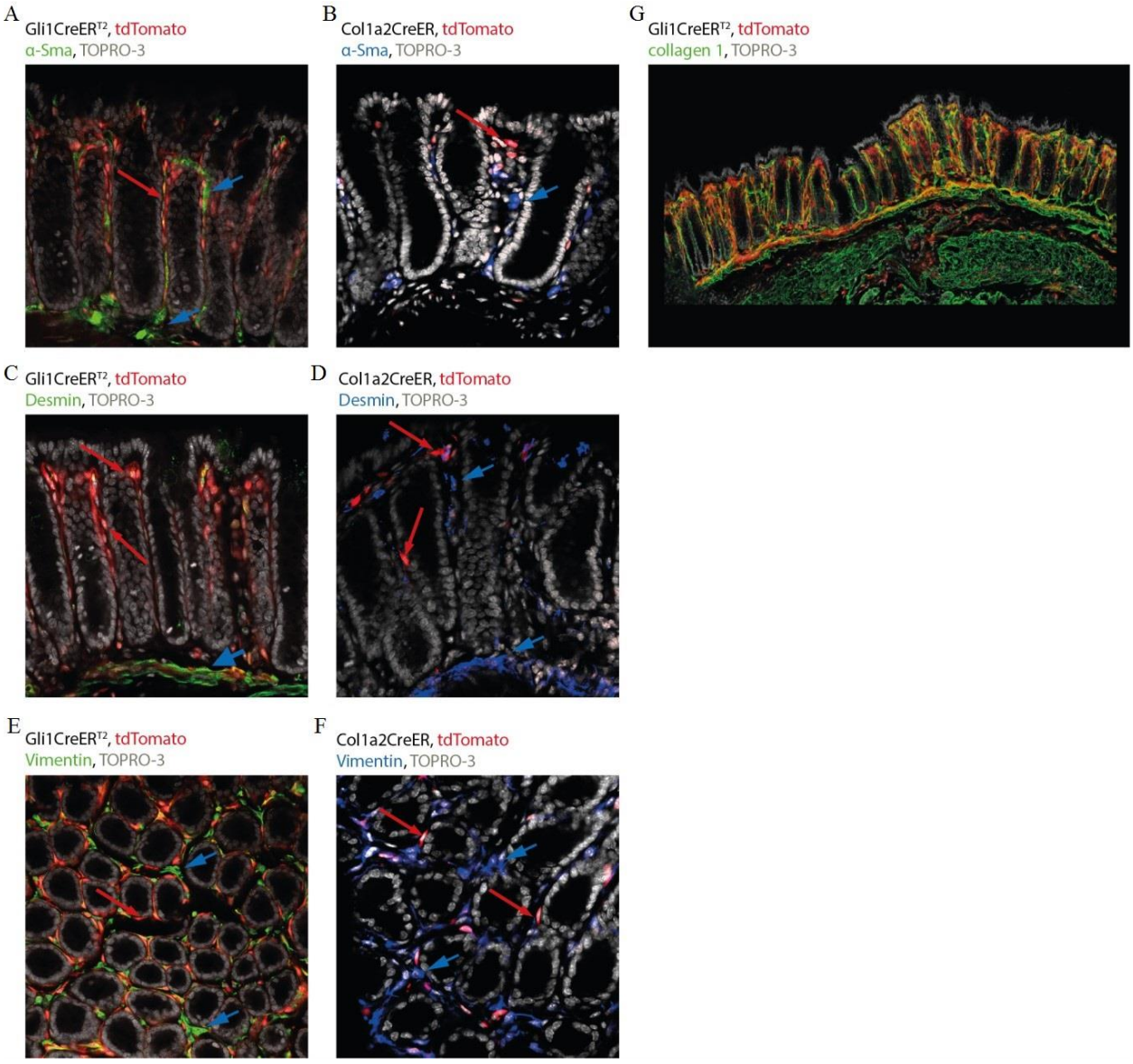

Figure 11. Confocal images combined with immunofluorescence against the stromal markers α-Sma, desmin or vimentin of *Gli1CreER^{T2};Rosa26-LSL-tdTomato* and *Col1a2CreER;R26-LSL-tdTomato* mice.

Red arrow indicates tomato$^+$ cell, blue arrow indicating either α-Sma$^+$, desmin$^+$ or vimentin$^+$ positive cell; TOPRO-3 was used as nuclear stain. (a) *Gli1CreER; R26-LSL-tdTomato* mouse and (b) *Col1a2CreER; R26-LSL-tdTomato* mouse stained for α -Sma; (c) *Gli1CreER; R26-LSL-tdTomato* mouse and (d) *Col1a2CreER; R26-LSL-tdTomato* mouse stained for desmin; (e) *Gli1CreER; R26-LSL-tdTomato* mouse and (f) *Col1a2CreER; R26-LSL-tdTomato* mouse stained for vimentin; (g) *Gli1CreER; R26-LSL-tdTomato* mouse stained for collagen1, yellow indicates overlap of Gli1 and Col1 [79].

5.7 Stromal Hedgehog pathway activation attenuates carcinogenesis upon AOM/DSS challenge

As we had shown that Hh activity is downregulated in AOM/DSS-derived colon tumors (Figure 8 & Figure 9) in areas of reduced Wnt pathway activity (Figure 10), we were interested in how stromal Hh activation would influence colonic carcinogenesis. To this end, we generated *Col1a2CreER;Ptch1*$^{fl/+}$ mice, which allow activation of Hh signaling exclusively in the stroma upon tamoxifen administration (Figure 4).

5.7.1 Increased *Gli1* expression upon stromal loss of one *Ptch1* allele

RT-qPCR analysis of *Gli1* mRNA expression showed a trend for an increase in the normal mucosa of *Col1a2CreER;Ptch1*$^{fl/+}$ mice compared to mucosa of littermate controls, although the difference did not reach the level of significance (Figure 12a). As for tumor tissue, *Gli1* mRNA expression was significantly higher in tumors of *Col1a2CreER;Ptch1*$^{fl/+}$ mice than in tumors of control mice (Figure 12b) [79].

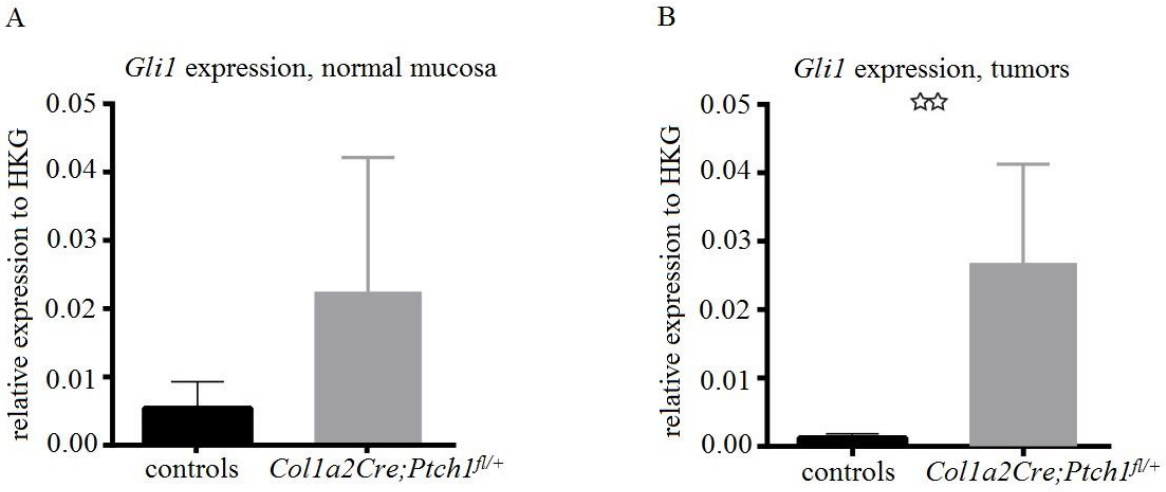

Figure 12. *Gli1* mRNA expression of *Col1a2Cre;Ptch1*$^{fl/+}$ and control mice without stromal Hedgehog activation. (a) Comparison of *Gli1* mRNA expression in normal mucosa of control mice and mice with Hh pathway activation. p = 0.24; n = 8 control mice and n = 6 *Col1a2Cre;Ptch1*$^{fl/+}$ mice. (b) Comparison of *Gli1* mRNA expression in tumors of control mice with tumors of *Col1a2Cre;Ptch1*$^{fl/+}$ mice. p = 0.002; n = 10 control mice and n = 9 *Col1a2Cre;Ptch1*$^{fl/+}$ mice (for both unpaired t-test of ΔCT values; **p ≤ 0.01). [79]

5.7.2 Fewer and smaller tumors upon Hedgehog pathway activation

Upon AOM/DSS challenge, *Col1a2CreER;Ptch1$^{fl/+}$* mice developed significantly fewer tumors compared to controls (Figure 13a). Furthermore, tumors in *Col1a2CreER;Ptch1$^{fl/+}$* mice were significantly smaller in size than in the control group (Figure 13b) [79].

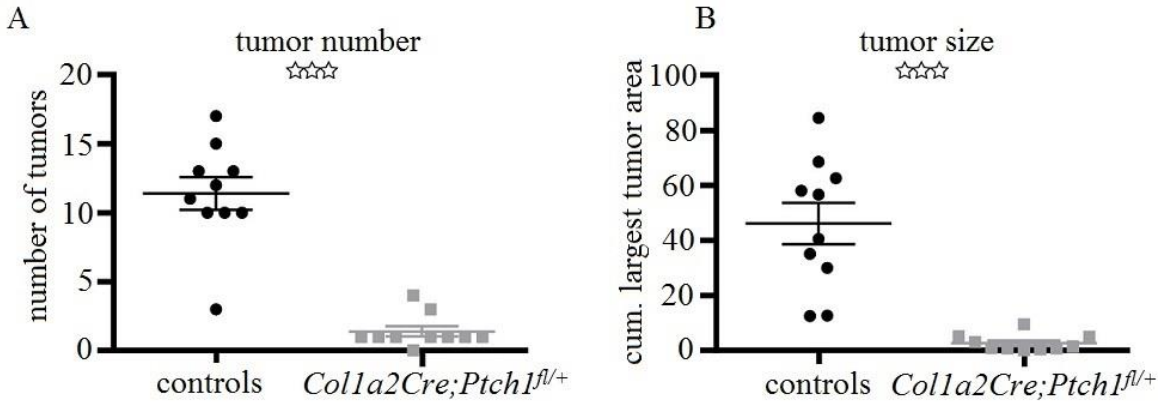

Figure 13. Tumor number and size of AOM/DSS-treated controls and *Col1a2Cre;Ptch1$^{fl/+}$* mice.

Comparison of tumor number (a) and size (b) in controls and mice with Hh pathway activation after AOM/DSS treatment. (a) Tumor number. Controls (n = 10) and *Col1a2Cre;Ptch1$^{fl/+}$* mice (n = 10); $p < 0.0001$ (b) Tumor size (cumulative area in mm^2 as assessed by small animal ultrasound). $p < 0.0001$ (for both unpaired t-tests, ***$p \leq 0.001$)[79]

5.8 Decreased PROX1 expression in lesions of *Col1a2CreER;Ptch1$^{fl/+}$* mice

The transcription factor PROX1 is a Wnt target gene specifically expressed in neoplastic colon cells [93]. As such, PROX1 expression can be used as a marker for malignant cells with high Wnt pathway activity and PROX1 expressing epithelial foci can be seen in dysplastic areas and overt tumors. We assessed PROX1 expression with IHC upon Hh activation in tumors and PROX1 expressing foci of *Col1a2CreER;Ptch1$^{fl/+}$* mice compared to controls. The average PROX1 intensity per individual lesion was significantly decreased in *Col1a2CreER;Ptch1$^{fl/+}$* mice compared to controls (Figure 14).

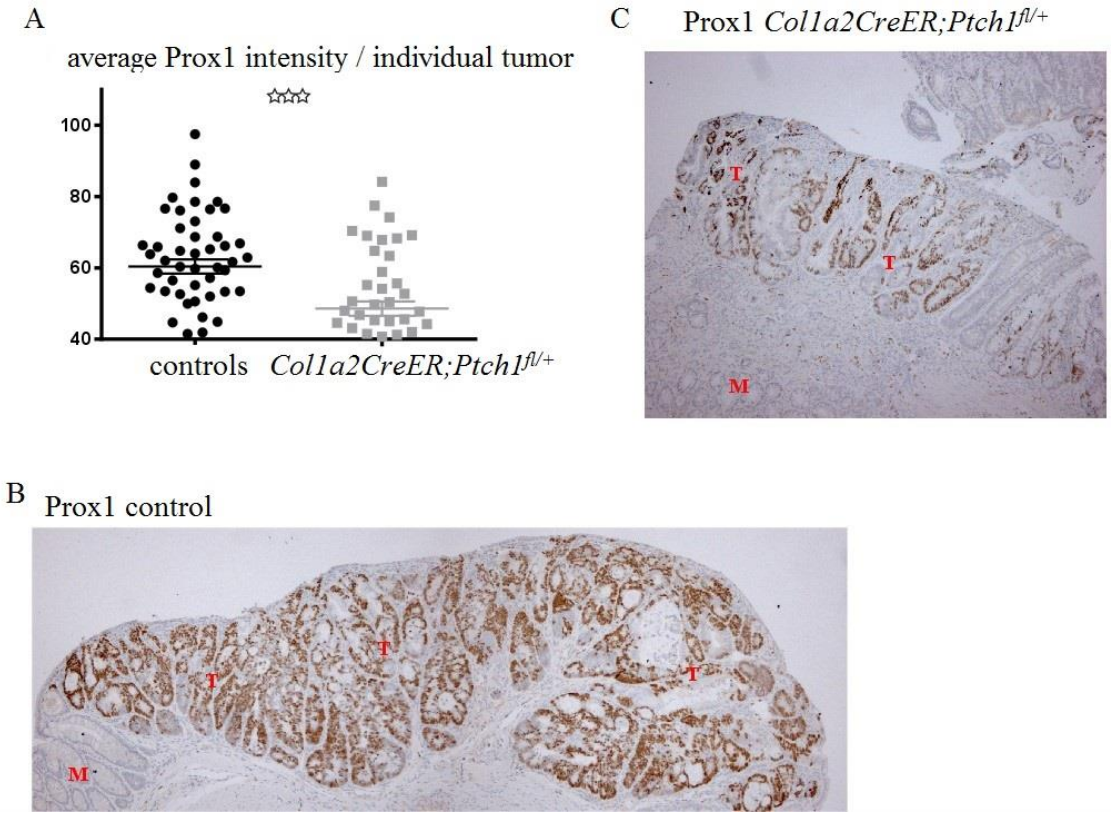

Figure 14. Prospero homeobox 1 protein expression in mice with Hedgehog activation and control mice.
(a) Quantification of PROX1 intensity (y-axis, intensity on 8-bit scale) per individual lesion of *Col1a2CreER;Ptch1$^{fl/+}$* and control mice. $p < 0.0001$ (unpaired t-test, ***$p \leq 0.001$). (b) Representative example of PROX1 IHC of a tumor in a control mouse; brown color indicating positive PROX1 staining. (c) Representative example of PROX1 IHC of a tumor in a *Col1a2CreER;Ptch1$^{fl/+}$* mouse; brown color indicating positive PROX1 staining, brown color indicating positive PROX1 staining. (T: Tumor; M: Mucosa)

5.9 Reduced tumor burden in a sporadic colorectal cancer model in mice with active stromal Hedgehog signaling

To investigate the effect of Hh activation in a model of sporadic colorectal carcinogenesis, we used a protocol based on repeated AOM injections without DSS to induce tumors in *Col1a2CreER;Ptch1*$^{fl/+}$ mice and littermate controls (Neufert 2007). *Col1a2CreER;Ptch1*$^{fl/+}$ mice challenged with AOM developed fewer tumors and tumors with a significantly smaller volume compared to the control group (Figure 15a&b) [79].

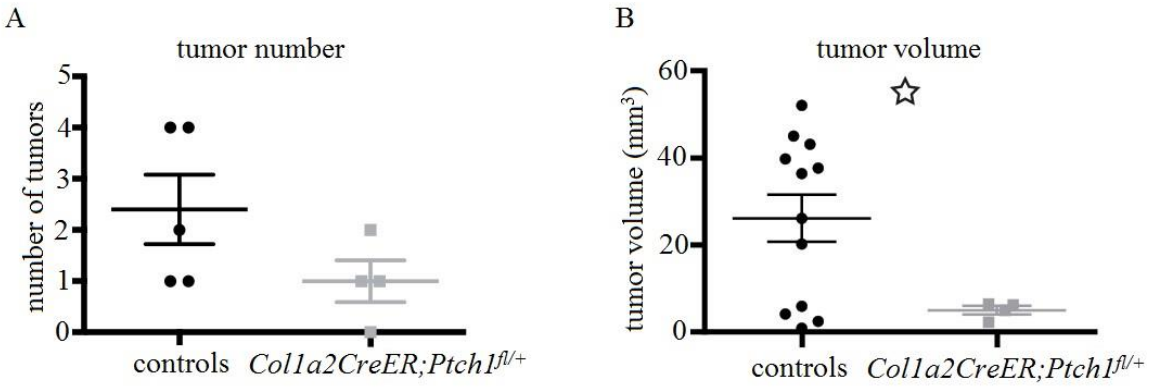

Figure 15. Tumor numbers and volumes for azoxymethane treated *Col1a2CreER;Ptch*$^{fl/+}$ mice and controls. Comparison of tumor number (a) and tumor volume as assessed with 3D ultrasound (b) after AOM treatment in control mice and mice with Hh pathway activation. (a) Tumor number. p = 0.143. (b) Tumor volume. p = 0.045 (controls: n = 5 mice; *Col1a2CreER;Ptch*$^{fl/+}$ mice: n = 4 that reached the endpoint , unpaired t-test, *p ≤ 0.05) [79].

5.10 P-Smads1/5 expression correlates with *Gli1* expression in AOM/DSS-derived colorectal cancers

Since BMP signaling triggers differentiation in colonic stem cells as well as in CRC stem cells, and because BMP expression is regulated by Hh signaling [94,95], we sought to investigate if Hh pathway activity correlates with downstream activity of the BMP pathway. Protein expression of p-SMADs1/5 indicates active BMP signaling. Therefore, we stained tumors in *Gli1*$^{lacZ/+}$mice immunohistochemically for p-SMADs1/5. IHC for p-SMADs1/5 of tumors induced in *Gli1*$^{lacZ/+}$ mice showed expression of p-SMADs1/5 that spatially correlated with high Gli1 expression in the stroma (Figure 16a). Quantitative analysis confirmed that p-SMADs1/5 immunoreactivity is significantly increased at the *Gli1*-expressing tumor periphery (Figure 16b).

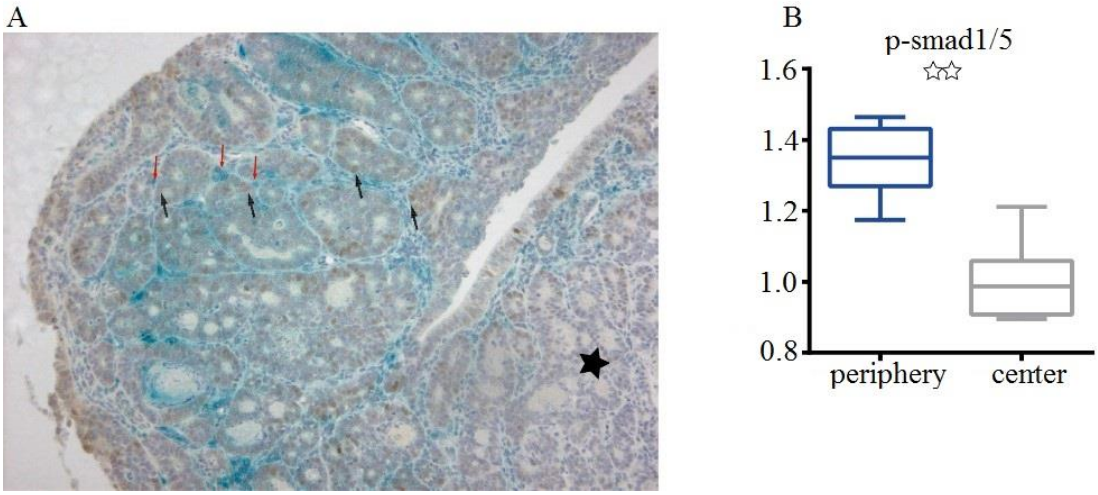

Figure 16. p-Smads 1/5 expression in *Gli1*$^{lacZ/+}$ tumors.

(a) IHC of p-SMADs1/5 in an X-gal-stained *Gli1*$^{lacZ/+}$ tumor. Blue color indicates a positive X-gal staining; brown color indicates positive DAB staining of p-SMADs1/5 expressing cells. Black arrows indicate positive p-SMADs1/5 staining's (brown); red arrows indicate positive X-gal staining (blue), asterisk indicates tumor center, where both p-SMAD1/5 and X-gal staining was weak to absent. (b) Quantification intensity in tumor periphery and center of p-SMADs1/5 stainings. Y-axis shows the relative staining intensity. n = 6 tumors, p = 0.0002, unpaired t-test [79].

5.11 *Bmp4* and *Bmp5* mRNA expression in AOM/DSS-induced tumors

Based on the data, supporting an association of the Hh pathway activity and the BMP-p-SMAD1/5 axis, we sought to confirm our findings by analyzing *Bmp4* and *Bmp5* mRNA expression in the same tumors that were used for the *Gli1* mRNA expression analysis. We compared the expression patterns of *Bmp4* and *Bmp5* in tumors and normal mucosa. The analysis of *Bmp4* mRNA expression in tumors compared to normal mucosa showed a significant up-regulation in the tumors (Figure 17a), while *Bmp5* expression was not significantly changed (Figure 17b).

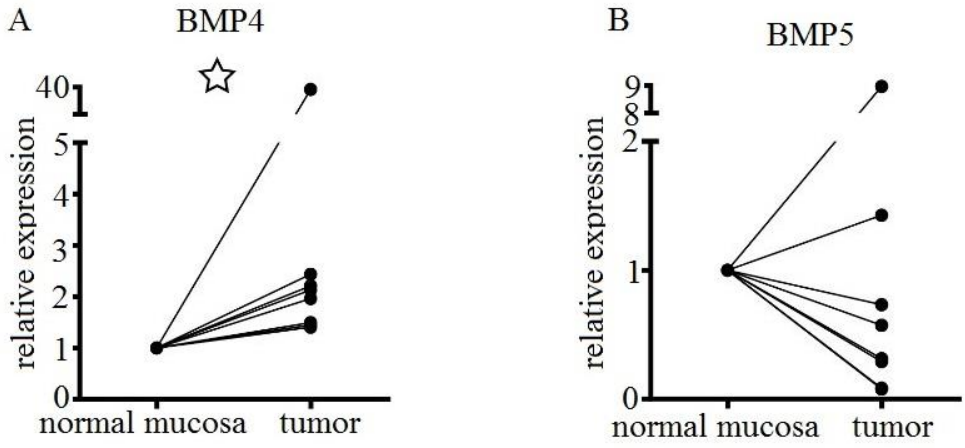

Figure 17. RT-qPCR for *Bmp4* and *Bmp5* mRNA expression of AOM/DSS-induced tumors and matched mucosa. Comparison of *Bmp4* (a) and *Bmp5* (b) mRNA expression in normal mucosa compared to that in AOM/DSS-induced tumors relative to the housekeeping gene. (a) BMP4 expression ($p = 0.0393$) (b) BMP5 expression ($p = 0.2323$) (both: $n = 8$ tumors and adjacent mucosa from 8 mice, paired t–test on ΔCT values, $*p \leq 0.05$)

5.12 α-Sma, desmin and vimentin protein expression upon Hedgehog activation

Since recent publications [96] described changes in the expression of the stroma markers α-Sma and desmin upon loss of Hh signaling in the small intestine, we were interested in how Hh activation would influence the stromal cell composition as defined by these markers. To this end, we first compared the changes following Hh activation in normal mucosa of *Col1a2CreER;Ptch1*$^{fl/+}$ mice with control mice and subsequently analyzed the changes in tumors of these mice.

5.12.1 Alteration of vimentin protein expression in normal mucosa upon stromal Hedgehog activation

Neither quantification of α-Sma nor of desmin IHC revealed significant differences between the mucosa of *Col1a2CreER;Ptch1*$^{fl/+}$ and controls (Figure 18a&b). However, quantification of

vimentin indicated a significant downregulation in *Col1a2CreER;Ptch1$^{fl/+}$* mice compared to controls (Figure 18c).

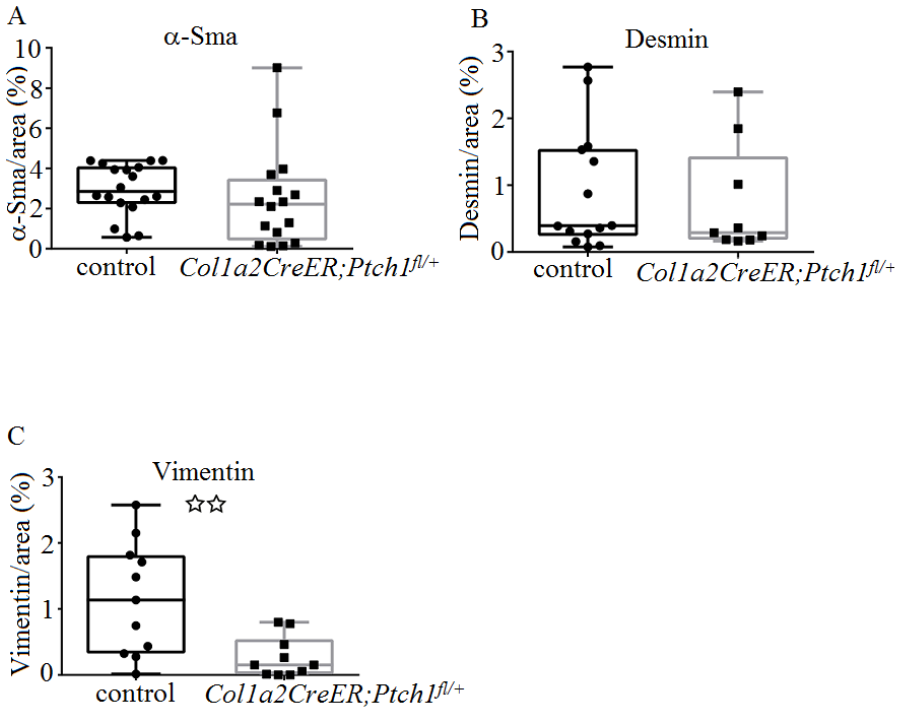

Figure 18. Quantification of α-Sma, desmin, and vimentin IHC of control mice mucosa vs. *Col1a2CreER;Ptch1$^{fl/+}$* mice mucosa.

Quantification of the difference in intensity between control mice and *Col1a2CreER;Ptch1$^{fl/+}$* mice mucosa for α-Sma: p = 0.5047 (a), desmin: p = 0.6623 (b) and vimentin: p = 0.0061 (c). Y-axis shows the percentage of the stained mucosal areas in relation to the overall area covered by the mucosa (all unpaired t-test, **p ≤ 0.01)

5.12.2 Desmin protein expression in tumors is changed upon stromal Hedgehog activation

Upon Hh pathway activation in *Col1a2CreER;Ptch1$^{fl/+}$* mice, we detected significant changes between the tumor stroma of mice with activated Hh signaling compared to the control group in terms of desmin protein abundance (Figure 19c). However, neither α-Sma nor vimentin protein expression were significantly different (Figure 19a&b). While the quantification of α-Sma showed a trend for up-regulation in tumors with activated Hh signaling compared to the controls, the quantification of vimentin showed a non-significant decrease in Hh-activated tumors compared to the control group.

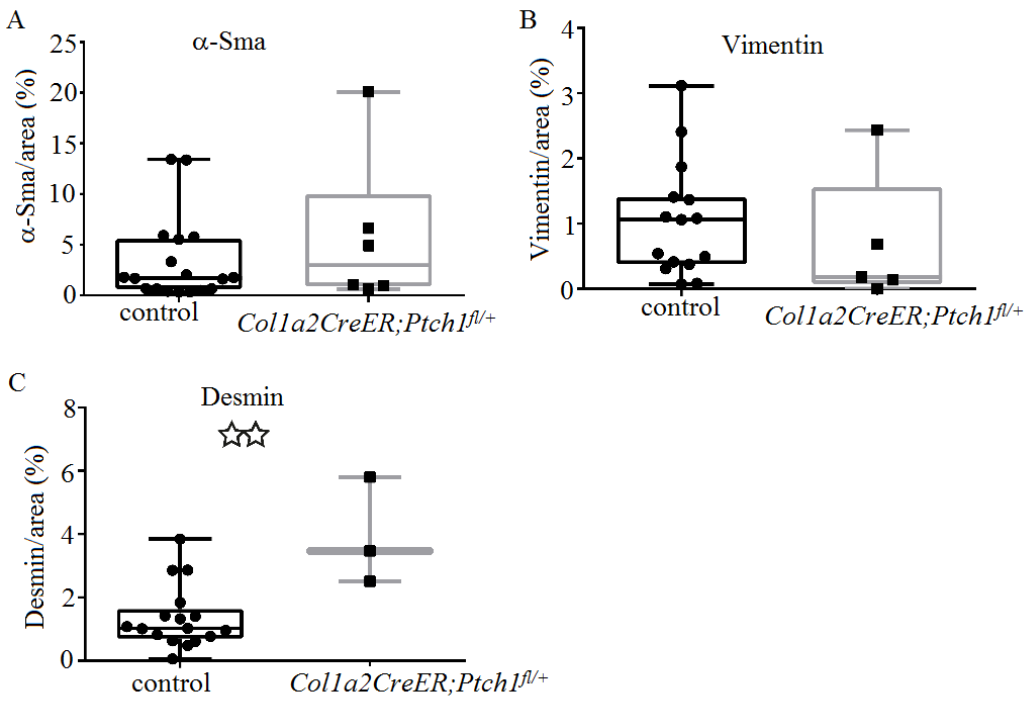

Figure 19. Quantification of α-Sma, vimentin, and desmin stainings of control mice tumors vs. *Col1a2CreER;Ptch1$^{fl/+}$* tumors.

Quantification of the difference in intensity between control mice and *Col1a2CreER;Ptch1$^{fl/+}$* mice tumors for α-Sma: p = 0.3287 (a); vimentin: p = 0.4560 (b); and Desmin: p = 0.0014 (c). Y-axis shows the percentage of the stained mucosal areas in relation to the overall area covered by the mucosa (all unpaired t-test, **p ≤ 0.01)

5.13 Reduced expression of Bone morphogenic pathway inhibitors upon Hedgehog activation

In the stroma of *Col1a2CreER;Ptch1$^{fl/fl}$* mice (homozygous floxed *Ptch1*), tamoxifen administration leads to “supramaximal” activation of the Hh pathway. We used this model for global gene expression analysis with microarray technology and applied GSEA [85] to rank the list of differentially expressed genes. The list of genes with the highest scores for down- or up-regulation after stromal Hh activation confirmed the Hh targets *Gli1*, *Ptch2* and *Hhip* among the top up-regulated genes (Figure 20a). Furthermore, GSEA displayed an enrichment of the canonical Hh pathway (gene set derived from MSigDB, gene set name: PID_HEDGEHOG_2PATHWAY) in Hh-activated mice versus controls (Figure 20b).

While stromal Hh activity correlated spatially with epithelial p-SMAD1/5 expression and thus with activation of downstream BMP signaling in the epithelium, our data on BMP ligand expression (BMP4 and BMP5) was inconclusive. Yet, downstream BMP signaling is modified by multiple BMP inhibitors, some of which have been shown to correlate with Hh activity [97]. Therefore, we were interested in how Hh activation influences BMP inhibitor expression. For this purpose, we analyzed the expression of a gene set of BMP inhibitors, including amongst others *Grem1*, Noggin (*Nog*), Chordin-like (*Chrld),* and BMP and activin membrane-bound inhibitor homolog (*Bambi*), using GSEA (gene set derived from gene ontology [GO] term “negative regulation of BMP signaling pathway"). Interestingly, GSEA revealed downregulation of a set of BMP inhibitors following Hh pathway up-regulation (Figure 20b).

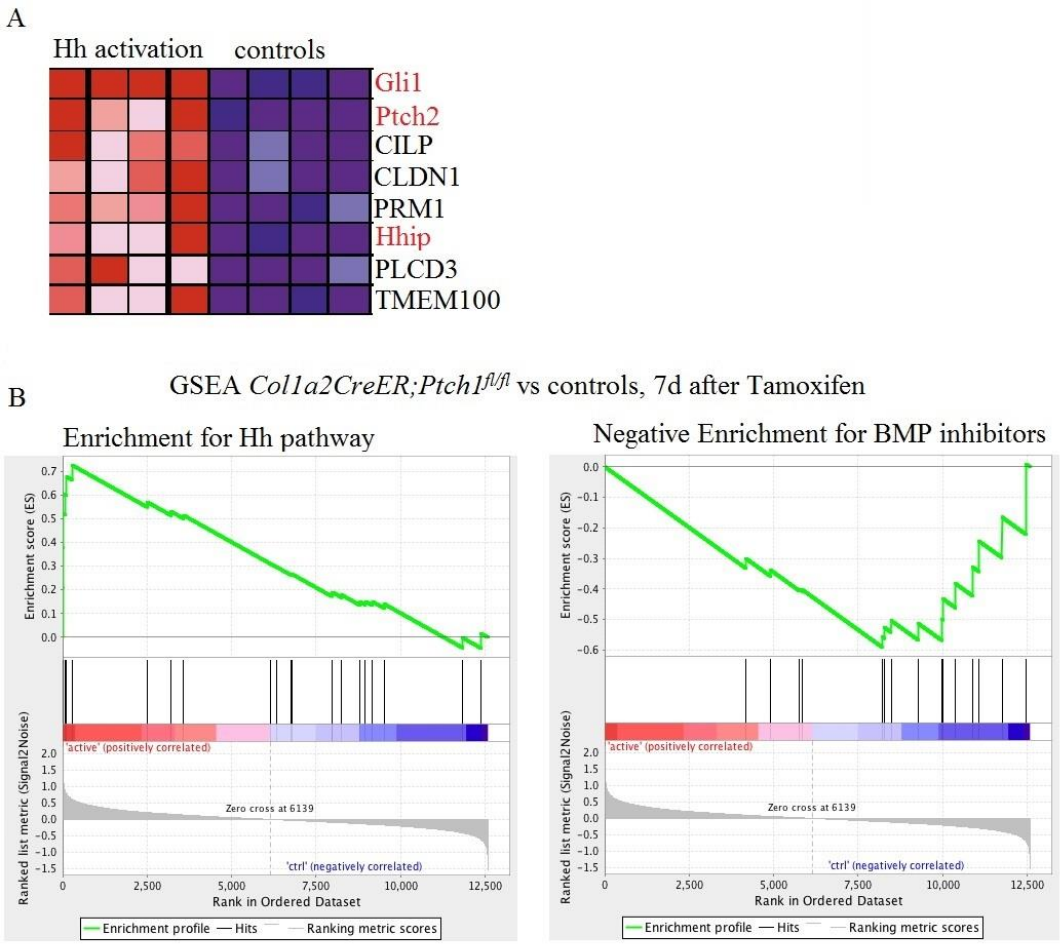

Figure 20. Gene expression microarray analysis of *Col1a2CreER;Ptch1$^{fl/fl}$* mice.

(a) Heatmap of the 8 highest ranked up-regulated genes in *Col1a2CreER;Ptch1$^{fl/fl}$* mice (Hh activated) vs. control mice. Red color indicates up-regulation and blue color down-regulation of the indicated genes. Hh pathway genes are red marked.

(b) GSEA for the Hh pathway (left) and for BMP inhibitors (right) in *Col1a2CreER;Ptch1$^{fl/fl}$* mice (n = 4) vs. controls (n = 4). Hh pathway: fdr = 0.001, normalized enrichment score (NES): 2.20, p = 0. BMP inhibitors: fdr = 0.092, NES = 1.67, p = 0.0106 [79]

5.14 Bone morphogenic protein pathway alterations upon Hedgehog activation *in vitro*

Based on the finding that BMP inhibitors are down-regulated upon Hh activation, we sought to confirm these results by analyzing if *in vitro* activation of Hh in stromal cells leads to similar expression patterns. We analyzed two GEO data sets (GSE29316 and GSE17840) [25,87], in which human colonic fibroblasts were treated with SHH protein, or murine intestinal mesenchymal cells with either IHH or SHH N-terminal polypeptide, respectively. In all cases, Hh activation led to up-regulation of *Gli1/GLI1*, confirming activation of downstream Hh signaling (Figure 21). Hh activation was paralleled to a significant down-regulation of the BMP inhibitor *Grem1/GREM1*

(Figure 21). While in the cultured intestinal mesenchyme, other BMP inhibitors were not significant down-regulated (Figure 21b), and the human colon fibroblast cell line showed a significant down-regulation of other BMP inhibitors such as *BAMBI*, *NOG*, *CHRLD1*, and *CHRD* (Figure 21a).

Since we found activation of downstream BMP signaling upon stromal Hh activity, and our data on BMP ligand expression was inconclusive, we revisited BMP ligand mRNA expression upon Hh activation *in vitro* in the public datasets. Again, we found a significant down-regulation of *BMP4* in the human cell line upon Hh activation (Figure 21a), while the cultured mesenchyme showed no significant changes in either *Bmp4* or *Bmp5* expression (Figure 21b).

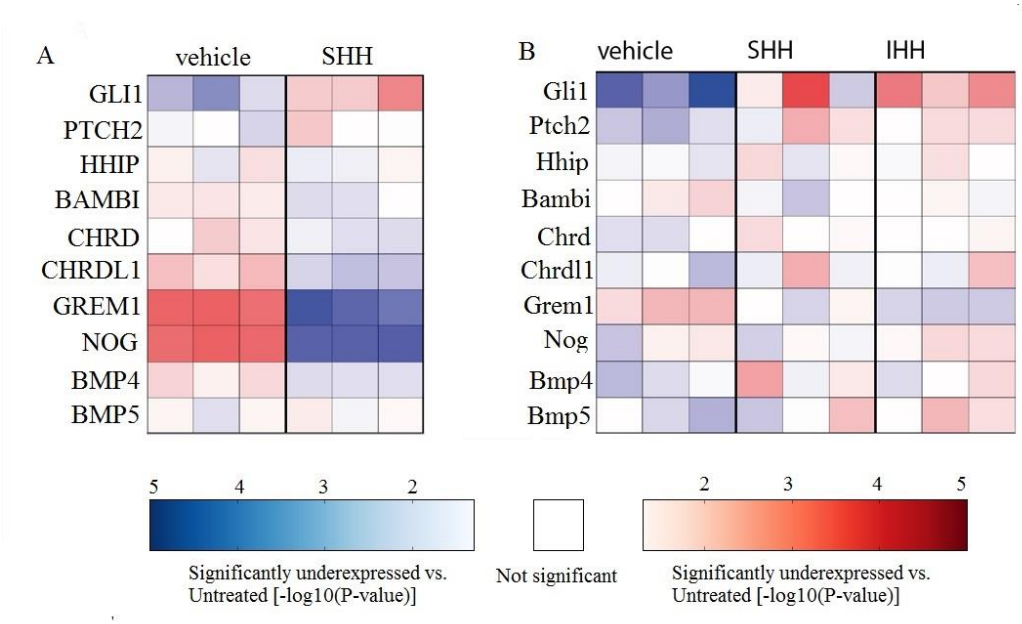

Figure 21. Gene expression upon Hedgehog activation *in vitro.*

(a) Gene expression of the indicated transcripts in a human colon fibroblast cell line (CCD-18Co) treated with 1µg/ml SHH or vehicle for 72 h [87]. Red color indicates high expression; blue colour indicates low expression. (b) Gene expression of indicated transcripts in cultured intestinal mesenchyme from E18.5 mouse embryos treated either with IHH, SHH N-terminal polypeptide (2.5 µg/ml) or vehicle for 24 h [25].

5.15 Bone morphogenetic protein inhibitor down-regulation upon Hedgehog pathway activation

In light of the findings that BMP inhibitors are down-regulated following Hh activation both *in vivo* and *in vitro*, we sought to validate if the tumors derived from heterozygous *Col1a2CreER;Ptch1*$^{fl/+}$ mice have a similar pattern of BMP inhibitor expression, which could possibly explain the relationship of stromal Hh expression with epithelial BMP induction. To this end, we performed RT-qPCRs on tumors of *Col1a2CreER;Ptch1*$^{fl/+}$ and control mice for 5 BMP inhibitors (*Bambi*, *Chrd*, *Grem1*, *Nog* and *Chrld1*) and compared their expression. We found that *Grem1* was significantly down-regulated (Figure 22).

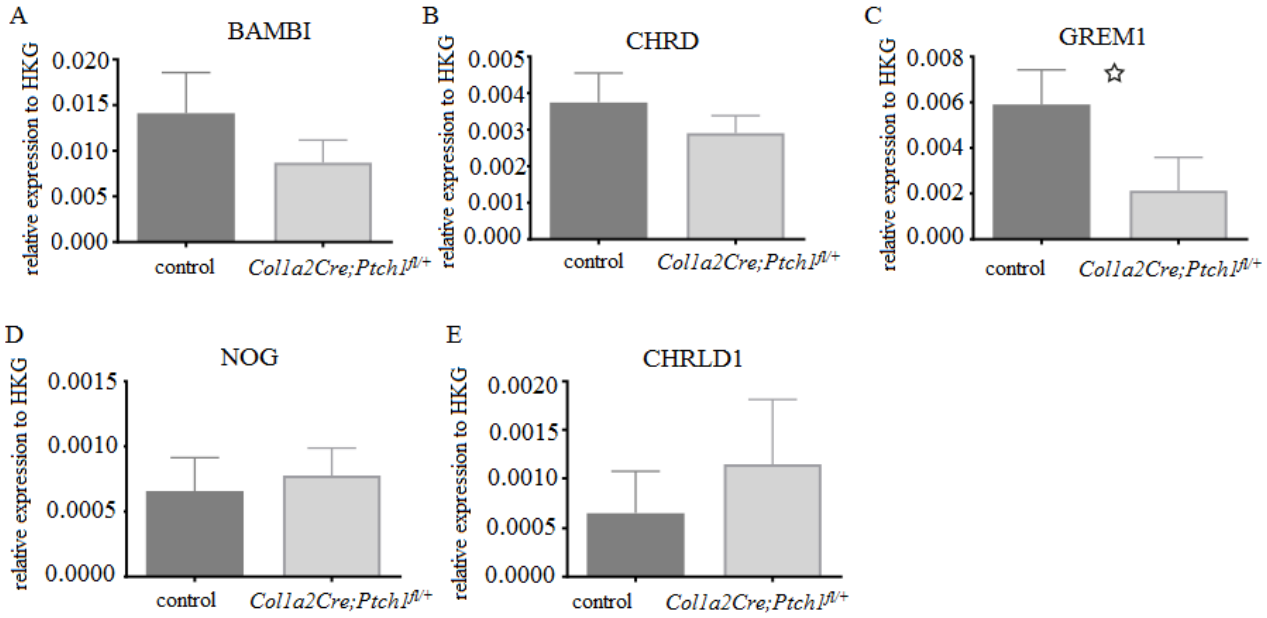

Figure 22. BMP inhibitor mRNA expression of Hedgehog pathway activated tumors compared to control tumors. RT-qPCR was used to assess mRNA expression of BMP inhibitors of tumors derived from *Col1a2Cre;Ptch1*$^{fl/+}$ mice (light grey) compared to control tumors (dark grey) relative to the HKG.
(a) *Bambi*: p = 0.484375. (b) *Chrd*: p = 0.484375. (c) *Grem1:* p = 0.0545. (d) *Nog:* p = 0.5823. (e) *Chrld1*: p = 0.484375. (n = 9 control mice and n = 10 *Col1a2Cre;Ptch1*$^{fl/+}$ mice; all unpaired t-tests on ΔCT values with multiple test correction, *p ≤ 0.05)

6 Discussion

6.1 Summary of the results

In some tumor types, autocrine, cell-autonomous Hh signaling acts as a driver of tumorigenesis. The classical example is basal cell carcinoma, which is almost exclusively driven by activation of Hh signaling in the tumor cells [55]. By contrast, no significant mutations were found in Hh-related genes in many other solid malignancies [54]. However, based on xenotransplantation studies, paracrine Hh signaling (from the tumor cells that produce the ligand to the receiving stroma translating the downstream signal) was found to promote tumor growth via microenvironmental cues [77]. Recently, this view has been challenged by novel animal models that found adverse outcomes after Hh inhibition in pancreatic and bladder cancer [62,63], as well as by clinical trials with Hh antagonists in, for example, colon and pancreatic cancer, which yielded no clinical benefit [59,98].

Therefore, the present study aimed to elucidate the effect of Hh alterations on CRC development, for which controversial data exist. Tumors of two chemically inducible tumor models (AOM/DSS or AOM only) for CRC in transgenic mice were analyzed to shed light on the role of Hh signaling for tumor-stroma crosstalk.

Firstly, by analysing mouse models that report Hh activity, we were able to show that Hh activity remains stromal and that downstream elements of the Hh pathway are down-regulated in murine colon tumors. Immunohistochemically, we found a connection between diminished stromal *Gli1* expression and areas of high Wnt pathway activity in the tumor cells. Moreover, the epithelial differentiation markers p-SMADs1/5, were locally enriched in close proximity to stromal cells with active Hh signaling, lending support to a pro-differentiating effect of stromal Hh pathway activation on the epithelial tumor cells. To explore this hypothesis functionally, we developed a mouse model to activate Hh signaling specifically in the stroma, by which we were able to identify a protective effect of Hh activation on colorectal carcinogenesis in chemically induced murine colonic tumors.

Gene expression microarray analysis pointed towards altered expression of BMP inhibitors as a mediator of this protective effect, an association that we could further confirm for the BMP inhibitor *Grem1 in vivo*.

6.2 Advantages and limitations of the study

6.2.1 The AOM/DSS and the AOM tumor models

Rodent animal models play an important role in research of intestinal neoplasia and are widely used to investigate pathways of tumor development and progression [99]. One of their general caveats in CRC research is the low frequency of invasiveness, a defining histologic feature of CRCs in humans [47]. While invasiveness beyond the *muscularis mucosae* and particularly distant metastases are largely absent in the majority of intestinal cancer mouse models, AOM/DSS-induced tumors do frequently show cytological features of malignancy, then referred to as "intramucosal adenocarcinomas", referring to neoplastic formations of cells that invade into the *lamina propria* or the *muscularis mucosae*, while the submucosa is not affected [48]. To investigate human CRCs, the administration of AOM/DSS or AOM to mice is a widely used model [91], as the murine CRCs show similarities to their human counterpart, such as their most common localization in the distal colon [67], their mutations leading to a Wnt pathway activation (such as *Apc* and *Ctnnb1* mutations) [100], and their *Kras* mutations [101]. Our results are consistent with these findings as we find activation of the Wnt pathway as indicated by mRNA expression analyses of *Lgr5* and *Axin2* (Figure 9), as well as nuclear translocation of β-catenin by IHC (Figure 10). However, it is important to emphasize that, for example, *p53* mutations, another hallmark in human CRC development, are rarely described in AOM/DSS-induced carcinomas [101,102].

One advantage of the administration of AOM combined with DSS is that the addition of DSS accelerates the growth of colon tumors dramatically compared to the exclusive administration of AOM [66]. Although the use of DSS can be beneficial for investigating inflammation-driven tumor progression (as, for example, ulcerative colitis or Crohn's disease have been associated with an increased risk for CRC [103]), the validity of transferring the results to sporadic tumors in patients without an inflammatory disease must be critically assessed. Mouse strain-dependent differences further complicate the interpretation of the results and their relation to human carcinomas [101]. Moreover, the murine diet as well as the immunologic status or bacterial colonization of the animals influence the metabolism of AOM, which adds another level of complexity when comparing results from different laboratories [104].

A further point to be considered is that the human colon tumors in general are a consequence of the exposure to carcinogens over a long period of time, whereas murine tumors arise from a high dose of a mutagenic agent during a very short time frame [101].

6.2.2 Immunohistochemistry

IHC is a well-established technique to assess protein expression *in situ* [105,106]. However, there are numerous different antibodies available, which differ in sensitivity and specificity. Regrettably, there exists neither a uniform threshold for positivity, nor a standard scoring system [106]. To quantify our results of DAB and X-gal stainings, we manually defined our regions of interest, which is a subjective approach, but cannot be fully avoided due to the nature of IHC [106].

6.3 Gene expression analysis

RT-qPCR and gene expression microarrays served to assess the expression levels of the Hh pathway, the Wnt pathway and some potentially involved pathways in the stroma-tumor crosstalk in tumors and normal mucosa of mice. RT-qPCR is a sensitive technique to analyze mRNA expression [107]. Optimized primers and reliable housekeeping genes as internal controls are critical requirements to gain results of high quality. Housekeeping genes should be expressed constitutively in all cells, independently of the experimental setting to be a good internal control [108]. We chose our main housekeeping gene, *Rplp0/ARP*, an acid ribosomal phosphoprotein, based on its characteristic as one of the most reliable housekeeping genes with constant expression levels in different cell types [109], as well as based on published data recommending *ARP* as a housekeeping gene especially for use in human bowel-inflammation and cancer research [110].

While qPCR is restricted to analyze only a handful of genes at a time, microarray analysis allows for screening a great number of genes simultaneously [111]. When interpreting array results, one should be aware that experimental artefacts can occur due to, for example, cross-hybridization between probes and the transcripts [112]. With the development of GSEA it became possible to assess sets of probes for enriched expression regarding, for example, a pathway of interest, hence leveling out some of the pitfalls when analyzing single genes [85].

6.4 The expression pattern of the Hedgehog pathway in the colon

While autocrine and paracrine Hh activation in CRC have been suggested [75,113], data on the normal colon clearly argue for a paracrine signaling mode [3,26,114], from differentiated enterocytes to stromal cells, such as smooth muscle cells, myofibroblasts or pericytes [3] (Figure 1). Previously, the assessment of Hh expression *in situ* has been challenging due to the lack of specific antibodies for downstream pathway members [77,115]. To circumvent this, we took advantage of a β-galactosidase knock-in to *Gli1* in *Gli1*$^{lacZ/+}$ mice to visualize Gli1 positive cells. In that way, we

were able to confirm a paracrine mode of signaling, as we observed the expression of Gli1, which is regarded the most robust indicator of downstream Hh signaling [116], exclusively in the stroma. To further assess Hh responsive cell populations, we stained *Gli1CreER^{T2};R26-LSL-Tomato* and *Col1a2CreER;R26-LSL-tdTomato* reporter mice for various stromal cell markers. The results confirm stromal exclusiveness of downstream Hh activity in the colon and furthermore suggest smooth muscle cells, pericytes or fibroblasts as Hh responsive cells (Figure 11). However, it was not possible to define a single specific cell population by one stromal cell marker alone as these markers are co-expressed by many different cells (Table 1).

6.5 The role of Hedgehog in chemically induced colorectal tumors

Previous data suggested a tumor-promoting role of the Hh pathway in human CRC [57,58], which, together with a body of *in vitro* data on Hh expression led to a clinical trial with the Hh inhibitor Vismodegib that, regrettably, yielded a negative result [59]. Hence, the role of Hh signaling for CRC development remained unclear.

6.5.1 Hedgehog Pathway regulation in AOM/DSS-induced colonic tumors

The data presented herein are in line with another study that used different mouse models to manipulate Hh signaling to reveal a protective effect of stromal Hh signaling on colorectal carcinogenesis [117]. Together with our data there is strong experimental support that Hh is protective in a variety of solid cancers, including pancreatic and bladder cancer [61,62].

We found down-regulation of stromal Gli1 expression in AOM/DSS-induced tumors using X-gal staining of whole-mount samples in *Gli1$^{lacZ/+}$* mice (Figure 7 & Figure 8), which could be confirmed on the mRNA level (Figure 9). At the same time, the tumors exhibited up-regulation of *Axin2*, and *Lgr5*, indicating Wnt pathway activation. The fact that the tumors did not reveal any down-regulation in *Ptch1* and *Ihh* mRNA expression (Figure 9 f&g) might be due to the limited number of tumors analyzed, or to non-canonical mechanisms involved in the regulation of Hh signaling in CRC [118]. Mechanisms that could contribute to this effect include the down-regulation of the Hh pathway co-receptors CDO, BOC and GAS1 [119], as they support the attenuation of the inhibitory effect of PTCH1 towards SMO upon Hh ligand binding in the canonical Hh pathway. Another explanation as to why *Ptch1* might not be down-regulated in tumors could be found in its role as a pro-apoptotic receptor in the epithelial compartment [120]. Here, bound Hh ligand might prevent apoptosis in tumor cells in a non-canonical manner [121]. As tumor formation results in the disruption of the normal mucosal structure, another reason for the dissociation between Hh ligands

and downstream Hh activity could be that the stromal ligand concentration is too low to activate downstream Hh signaling. This would be in line with previously published data demonstrating that stromal Hh pathway activation is a result of high Hh ligand concentrations at the villus tips, generated by folding of the epithelial during intestinal development [122].

6.5.2 Protective effect of Hedgehog on colorectal carcinogenesis

To activate the Hh pathway, we made use of *Col1a2CreER;Ptch1$^{fl/+}$* mice, which lose one *Ptch1* allele specifically in *Collagen1a2* expressing stroma cells upon tamoxifen administration. In both, the inflammation-driven (AOM/DSS) and sporadic (AOM) tumor model, we found a protective effect of Hh activation (Figure 13 & Figure 15). These findings support a model, in which stromal Hh signals have protective effects in the development of CRC. Furthermore, we were able to show that Hh activation leads to down-regulation of the tumor-promoting epithelial transcription factor protein PROX1 [93] (Figure 14), supporting the hypothesis of a pro-differentiating effect of stromal Hh activation.

The results of Hh down-regulation in colorectal tumors have to be put in context with increased Hh pathway activity in adenomas of patients with FAP reported earlier [96]. A possible explanation is that Hh pathway activity could be necessary for adenoma formation, as it was also shown earlier for *Apc^{min}* mice [96], but the Hh downstream signal is lost upon further progression to carcinomas. This would be in line with the finding that administration of Hh inhibitors to *Apc^{min}* mice bearing advanced adenomas resulted in bigger adenomas instead of growth restriction [96]. Apart from the structural and functional differences of these two tissues, such as the presence of villi or the existence of Paneth cells in the small intestine, recent data suggest that a higher number of oncogenic mutations is needed for tumor development in the murine colon compared to the small intestine [123]. In addition, *Apc^{min}*-driven tumors as well as FAP are based on a single mutation in the *APC* gene, whereas we made use of carcinogen-induced tumors, which are associated with a more complex mutation pattern [100,101], and which could explain parts of the differences observed.

6.6 Changes in stroma composition upon Hedgehog pathway alterations

The Hh pathway is known to play a crucial role in mesenchymal homeostasis of the adult intestine [3], and recent data suggest significant changes in the adenoma stroma upon Hh deactivation [124]. Therefore, we investigated the changes in stromal composition upon Hh activation of normal colon mucosa and of the tumor stroma in our mouse model, as potential changes in the tumor stroma

could also account for decreased tumor development and progression. Since changes in the stroma upon Hh activation occurred in the normal mucosa, we expected similar findings, such as an increase of α-Sma positive cells, in the tumors [10]. Interestingly, we found a decrease in vimentin protein abundance, but no significant changes in the stroma markers α-Sma or desmin in the normal mucosa of the Hh-activated *Col1a2CreER;Ptch1*$^{fl/+}$ mice compared to control mice.

A possibility for the limited changes upon the loss of one *Ptch1* allele could be that the loss of one allele does not result in a sufficiently strong Hh pathway up-regulation to cause fundamental changes in the stromal cell composition. Again, it should be emphasized that we analyzed the colonic stroma, while Büller *et al.* focused on the small intestine, which could explain why there is a different response upon Hh alterations of the stroma. When looking at the expression of α-Sma, vimentin, and desmin in tumors with Hh-activated stroma compared to tumors of control mice, we found a significant up-regulation of desmin, but no other fibroblast markers. This would be in line with Büller *et al*., who described a loss of desmin and α-Sma positive cells upon the loss of Hh signaling [124].

6.7 The Hedgehog-Bone morphogenetic protein axis: a potential link of the protective role of Hedgehog in colorectal carcinogenesis

Given that Hh signaling activity is decreased in CRC, and stromal Hh activation can act in a protective manner on colonic tumor development, we sought to elucidate mechanistic links between stromal Hh activation and epithelial differentiation. The BMP pathway has a pro-differentiating effect on the intestinal epithelium, restrains the stem cell compartment [125] (Figure 1) and, importantly, is driven by active Hh signaling [3,126]. Together with recent investigations by Shin *et al*, which addressed the Hh-BMP axis in bladder cancer, this prompted us to investigate the Hh-BMP axis in our study [63].

Firstly, we were able to identify a correlation between stromal expressed Gli1 and the expression of p-SMADs1/5 (Figure 16). As the phosphorylation of SMADs1/5 occurs downstream of Bmp ligands, our findings support a model of Ihh-driven stromal Bmp activation [33]. Furthermore, as the Bmp pathway induces intestinal differentiation and acts as a Wnt pathway antagonist [9], these findings support the hypothesis of Hh-BMP-driven tumor suppression. Motivated by these results, we sought to confirm the association between the Hh pathway and the BMP-p-SMADs1/5 axis by analyzing *Bmp4* and *Bmp5* mRNA expression in AOM/DSS-induced tumors. While *Bmp5* expression showed a trend for down-regulation in the tumors, the anticipated down-regulation of

Bmp4, in accordance to the down-regulation of *Gli1*, could not be confirmed. Unexpectedly, the results even demonstrated an increase of *Bmp4* mRNA expression, as it was also reported in adenomas of the small intestine [124]. It might be possible that *Bmp4* and *Bmp5* follow different regulatory mechanisms during tumor progression. Furthermore, other factors could activate the BMP pathway (especially *Bmp4*) independent of Hh signaling, also in the epithelial cell compartment [95].

To investigate further the mechanisms of how Hh-BMP signaling might restrain colorectal carcinogenesis, we analyzed the expression patterns of BMP inhibitors upon Hh activation. BMP inhibitors are major stem cell niche factors (Figure 1) and may trigger carcinogenesis in the colon [34]. We found that BMP inhibitor expression is down-regulated upon Hh pathway activation. These results further support the hypothesis of a connection between BMP pathway up-regulation (in this case via a reduction of BMP suppression), induced by Hh activity. To verify our hypothesis of BMP inhibitor down-regulation upon stromal Hh activation, we analyzed two *in vitro* gene expression data sets for the expression of BMP ligands and BMP inhibitors upon stromal Hh activation. In both cases, we found significant down-regulation of the BMP inhibitor *Grem1* upon Hh activation, emphasizing *Grem1* as a main factor, associated with tumor growth restriction upon Hh activation. Next, we sought to confirm these findings by comparing tumors of *Col1a2Cre;Ptch1*$^{fl/+}$ mice, which revealed increased *Gli1* expression, with tumors of control mice. Regarding Hh-activated tumors, we found ambiguous results, as two inhibitors (*Nog* and *Chrld1*) showed a slight increase, while *Bambi*, *Chrd*, and *Grem1* indicated decreased expression, which might be due to the limited number of tumors analyzed or it could be that not all BMP inhibitors have the same impact on tumor formation. Focusing on *Grem1*, which plays a role for colon tumor formation in animal models [34] as well as in human CRC [127,128], our results together with these data imply a tumor-protective role of Hh activation via the reduction of BMP inhibitors, especially *Grem1* (Figure 23*)*.

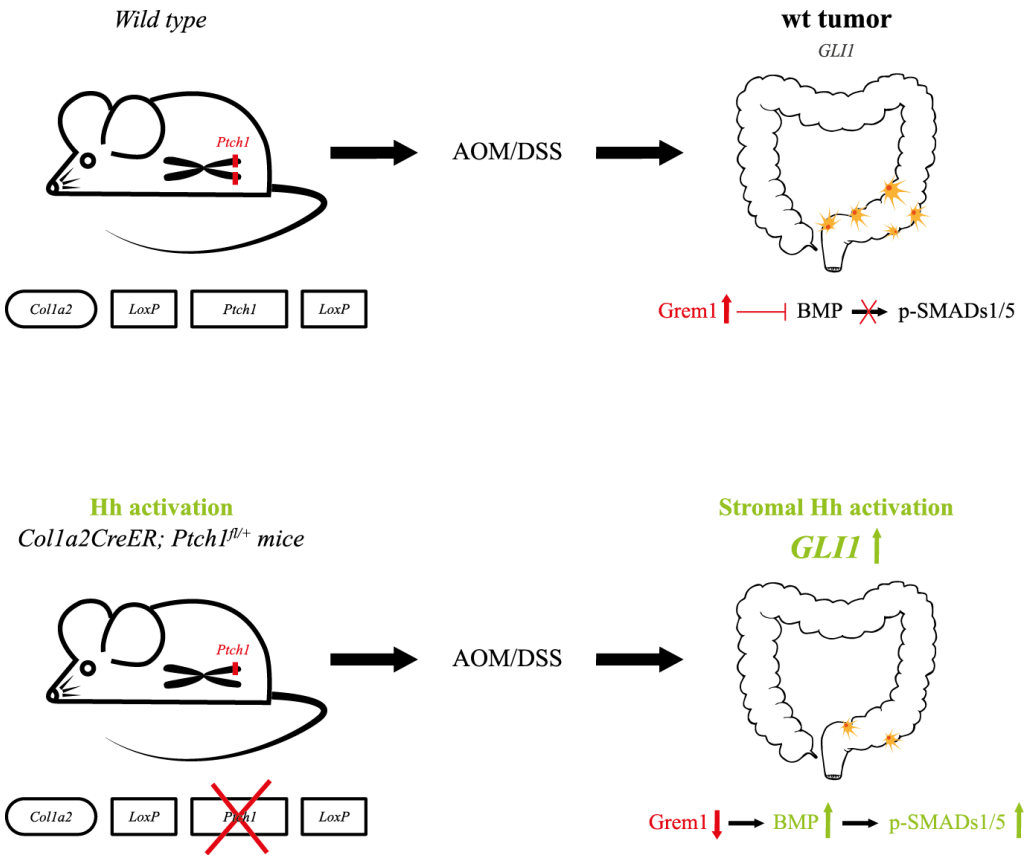

Figure 23. Protective effect of stromal Hedgehog activation on colorectal cancer development.

In our study, Hh activation in *Col1a2Cre;Ptch1*$^{fl/+}$ mice had a protective effect on AOM/DSS-induced CRC development. Our results suggest that Hh activation (high *Gli1* expression) acts via the Hh-BMP axis, particularly through repressed expression of BMP inhibitors such as *Grem1*.

7 Conclusion and clinical relevance

Our data are in line with recent publications suggesting a protective effect of Hh signaling in tumor growth of different cancer types [61–63]. At the same time, they challenge the common model of a tumor-promoting role of the stroma, and rather support a protective role, at least inf pancreatic-, bladder-, and colorectal cancer. Hh-driven changes emerge as important mediators for these protective effects of the stroma. The data furthermore suggest the Hh-BMP axis, via down-regulation of the BMP inhibitor *Grem1*, as a potential pathway behind the tumor suppressing effects (Figure 23). Further clarification of the role of this stroma-tumor crosstalk in CRC devolvement could lead to the identification of pharmacological targets in the stroma to treat CRC.

8 References

1. Sancho, E., Batlle, E. & Clevers, H. Signaling Pathways in Intestinal Development and Cancer. *Annu. Rev. Cell Dev. Biol.* 20, 695–723 (2004).
2. Tortora, G. J. & Derrickson, B. H. Principles of Anatomy and Physiology. 12th edition. John Wiley & Sons. 924-926 (2008).
3. Büller, N. V. J. A., Rosekrans, S. L., Westerlund, J. & van den Brink, G. R. Hedgehog Signaling and Maintenance of Homeostasis in the Intestinal Epithelium. *Physiology* 27, 148–155 (2012).
4. Helander, H. F. & Fändriks, L. Surface area of the digestive tract – revisited. *Scand. J. Gastroenterol.* 49, 681–689 (2014).
5. van der Flier, L. G. & Clevers, H. Stem Cells, Self-Renewal, and Differentiation in the Intestinal Epithelium. *Annu. Rev. Physiol.* 71, 241–260 (2009).
6. Barker, N., van Es, J. H., Kuipers, J., Kujala, P., van den Born, M., Cozijnsen, M., Haegebarth, A., Korving, J., Begthel, H., Peters, P. J. & Clevers, H. Identification of stem cells in small intestine and colon by marker gene Lgr5. *Nature.* 449, 1003–1007 (2007).
7. Egeblad, M., Nakasone, E. S. & Werb, Z. Tumors as organs: complex tissues that interface with the entire organism. *Dev. Cell*. 18, 884–901 (2010).
8. Mifflin, R. C., Pinchuk, I. V., Saada, J. I. & Powell, D. W. Intestinal myofibroblasts: targets for stem cell therapy. *Am. J. Physiol. - Gastrointest. Liver Physiol.* 300, G684–G696 (2011).
9. Powell, D. W., Pinchuk, I. V., Saada, J. I., Chen, X. & Mifflin, R. C. Mesenchymal Cells of the Intestinal Lamina Propria. *Annu. Rev. Physiol.* 73, 213–237 (2011).
10. Zacharias, W. J., Madison, B. B., Kretovich, K. E., Walton, K. D., Richards, N., Udager, A. M., Li, X. & Gumucio, D. L. Hedgehog signaling controls homeostasis of adult intestinal smooth muscle. *Dev. Biol.* 355, 152–162 (2011).

11. Minguell, J. J., Erices, A. & Conget, P. Mesenchymal Stem Cells. *Exp. Biol. Med.* 226, 507–520 (2001).

12. Öhlund, D., Elyada, E. & Tuveson, D. Fibroblast heterogeneity in the cancer wound. *J. Exp. Med.* 211, 1503–1523 (2014).

13. Serini, G., Bochaton-Piallat, M.-L., Ropraz, P., Geinoz, A., Borsi, L., Zardi, L. & Gabbiani, G. The Fibronectin Domain ED-A Is Crucial for Myofibroblastic Phenotype Induction by Transforming Growth Factor-β1. *J. Cell Biol.* 142, 873–881 (1998).

14. Tomasek, J. J., Gabbiani, G., Hinz, B., Chaponnier, C. & Brown, R. A. Myofibroblasts and mechano-regulation of connective tissue remodelling. *Nat. Rev. Mol. Cell Biol.* 3, 349–363 (2002).

15. Segditsas, S. & Tomlinson, I. Colorectal cancer and genetic alterations in the Wnt pathway. *Oncogene*. 25, 7531–7537 (2006).

16. Logan, C. Y. & Nusse, R. The Wnt Signaling Pathway in Development and Disease. *Annu. Rev. Cell Dev. Biol.* 20, 781–810 (2004).

17. van de Wetering, M., Sancho, E., Verweij, C., de Lau, W., Oving, I., Hurlstone, A., van der Horn, K., Batlle, E., Coudreuse, D., Haramis, A. P., Tjon-Pon-Fong, M., Moerer, P., van den Born, M., Soete, G., Pals, S., Eilers, M., Medema, R. & Clevers, H. The beta-catenin/TCF-4 complex imposes a crypt progenitor phenotype on colorectal cancer cells. *Cell.* 111, 241–250 (2002).

18. Ragusa, S., Cheng, J., Ivanov, K. I., Zangger, N., Ceteci, F., Bernier-Latmani, J., Milatos, S., Joseph, J.-M., Tercier, S., Bouzourene, H., Bosman, F. T., Letovanec, I., Marra, G., Gonzalez, M., Cammareri, P., Sansom, O. J., Delorenzi, M. & Petrova, T. V. PROX1 Promotes Metabolic Adaptation and Fuels Outgrowth of Wnthigh Metastatic Colon Cancer Cells. *Cell Rep.* 8, 1957–1973 (2014).

19. He, X. C., Zhang, J. & Li, L. Cellular and Molecular Regulation of Hematopoietic and Intestinal Stem Cell Behavior. *Ann. N. Y. Acad. Sci.* 1049, 28–38 (2005).

20. Miyazono, K., Kamiya, Y. & Morikawa, M. Bone morphogenetic protein receptors and signal transduction. *J. Biochem. (Tokyo)* 147, 35–51 (2010).

21. van den Brink, G. R. Hedgehog Signaling in Development and Homeostasis of the Gastrointestinal Tract. *Physiol. Rev.* 87, 1343–1375 (2007).

22. Corbit, K. C., Aanstad, P., Singla, V., Norman, A. R., Stainier, D. Y. R. & Reiter, J. F. Vertebrate Smoothened functions at the primary cilium. *Nature* 437, 1018–1021 (2005).

23. Walton, K. D., Kolterud, Å., Czerwinski, M. J., Bell, M. J., Prakash, A., Kushwaha, J., Grosse, A. S., Schnell, S. & Gumucio, D. L. Hedgehog-responsive mesenchymal clusters direct patterning and emergence of intestinal villi. *Proc. Natl. Acad. Sci.* 109, 15817–15822 (2012).

24. van Dop, W. A., Uhmann, A., Wijgerde, M., Sleddens–Linkels, E., Heijmans, J., Offerhaus, G. J., van den Bergh Weerman, M. A., Boeckxstaens, G. E., Hommes, D. W., Hardwick, J. C., Hahn, H. & van den Brink, G. R. Depletion of the Colonic Epithelial Precursor Cell Compartment Upon Conditional Activation of the Hedgehog Pathway. *Gastroenterology* 136, 2195–2203.e7 (2009).

25. Zacharias, W. J., Li, X., Madison, B. B., Kretovich, K., Kao, J. Y., Merchant, J. L. & Gumucio, D. L. Hedgehog Is an Anti-Inflammatory Epithelial Signal for the Intestinal Lamina Propria. *Gastroenterology* 138, 2368–2377.e4 (2010).

26. van Dop, W. A., Heijmans, J., Büller, N. V. J. A., Snoek, S. A., Rosekrans, S. L., Wassenberg, E. A., van den Bergh Weerman, M. A., Lanske, B., Clarke, A. R., Winton, D. J., Wijgerde, M., Offerhaus, G. J., Hommes, D. W., Hardwick, J. C., de Jonge, W. J., Biemond, I. & van den Brink, G. R. Loss of Indian Hedgehog Activates Multiple Aspects of a Wound Healing Response in the Mouse Intestine. *Gastroenterology* 139, 1665–1676.e10 (2010).

27. Lin, S. & Barker, N. Gastrointestinal stem cells in self-renewal and cancer. *J. Gastroenterol.* 46, 1039–1055 (2011).

28. Barker, N. Adult intestinal stem cells: critical drivers of epithelial homeostasis and regeneration. *Nat. Rev. Mol. Cell Biol.* 15, 19–33 (2013).

29. Yen, T.-H. & Wright, N. A. The gastrointestinal tract stem cell niche. *Stem Cell Rev.* 2, 203–212 (2006).

30. Kabiri, Z., Greicius, G., Madan, B., Biechele, S., Zhong, Z., Zaribafzadeh, H., Edison, Aliyev, J., Wu, Y., Bunte, R., Williams, B. O., Rossant, J. & Virshup, D. M. Stroma provides an intestinal stem cell niche in the absence of epithelial Wnts. *Development* dev.104976 (2014). doi:10.1242/dev.104976

31. Valenta, T., Degirmenci, B., Moor, A. E., Herr, P., Zimmerli, D., Moor, M. B., Hausmann, G., Cantù, C., Aguet, M. & Basler, K. Wnt Ligands Secreted by Subepithelial Mesenchymal Cells Are Essential for the Survival of Intestinal Stem Cells and Gut Homeostasis. *Cell Rep.* 15, 911–918 (2016).

32. Kosinski, C., Li, V. S. W., Chan, A. S. Y., Zhang, J., Ho, C., Tsui, W. Y., Chan, T. L., Mifflin, R. C., Powell, D. W., Yuen, S. T., Leung, S. Y. & Chen, X. Gene expression patterns of human colon tops and basal crypts and BMP antagonists as intestinal stem cell niche factors. *Proc. Natl. Acad. Sci.* 104, 15418–15423 (2007).

33. Vermeulen, L., Melo, F. D. S. E., van der Heijden, M., Cameron, K., de Jong, J. H., Borovski, T., Tuynman, J. B., Todaro, M., Merz, C., Rodermond, H., Sprick, M. R., Kemper, K., Richel, D. J., Stassi, G. & Medema, J. P. Wnt activity defines colon cancer stem cells and is regulated by the microenvironment. *Nat. Cell Biol.* 12, 468–476 (2010).

34. Davis, H., Irshad, S., Bansal, M., Rafferty, H., Boitsova, T., Bardella, C., Jaeger, E., Lewis, A., Freeman-Mills, L., Giner, F. C., Rodenas-Cuadrado, P., Mallappa, S., Clark, S., Thomas, H., Jeffery, R., Poulsom, R., Rodriguez-Justo, M., Novelli, M., Chetty, R., Silver, A.,

Sansom, O. J., Greten, F. R., Wang, L. M., East, J. E., Tomlinson, I. & Leedham, S. J. Aberrant epithelial GREM1 expression initiates colonic tumorigenesis from cells outside the stem cell niche. *Nat. Med.* advance online publication. (2014).

35. Ferlay, J., Soerjomataram, I., Dikshit, R., Eser, S., Mathers, C., Rebelo, M., Parkin, D. M., Forman, D. & Bray, F. Cancer incidence and mortality worldwide: Sources, methods and major patterns in GLOBOCAN 2012. *Int. J. Cancer* (2014).
36. Jemal, A., Bray, F., Center, M. M., Ferlay, J., Ward, E. & Forman, D. Global cancer statistics. *CA Cancer J. Clin.* 61, 69–90 (2011).
37. Robert Koch-Institut und die Gesellschaft der epidemiologischen Krebsregister in Deutschland e.V. *Krebs in Deutschland 2009/2010. 9. Ausgabe.* (2013).
38. Pox, C., Schmiegel, W. & Classen, M. Current status of screening colonoscopy in Europe and in the United States. *Endoscopy* 39, 168–173 (2007).
39. Deutsche Krebsgesellschaft, Deutsche Krebshilfe, & AWMF. Leitlinienprogramm Onkologie: S3-Leitlinie Kolorektales Karzinom, Kurzversion 1.1 , 2014, AW MF Registrierungsnummer: 021 -007OL. (2014). at <https://www.leitlinienprogramm-onkologie.de/leitlinien/kolorektales-karzinom/>
40. Vogelstein, B., Fearon, E. R., Hamilton, S. R., Kern, S. E., Preisinger, A. C., Leppert, M., Smits, A. M. M. & Bos, J. L. Genetic Alterations during Colorectal-Tumor Development. *N. Engl. J. Med.* 319, 525–532 (1988).
41. Michor, F., Iwasa, Y. & Nowak, M. A. Dynamics of cancer progression. *Nat. Rev. Cancer* 4, 197–205 (2004).
42. Arakawa, H. Netrin-1 and its receptors in tumorigenesis. *Nat. Rev. Cancer* 4, 978–987 (2004).
43. Fearon, E. R. Molecular Genetics of Colorectal Cancer. *Annu. Rev. Pathol. Mech. Dis.* 6, 479–507 (2011).

44. Fleming, M., Ravula, S., Tatishchev, S. F. & Wang, H. L. Colorectal carcinoma: Pathologic aspects. *J. Gastrointest. Oncol.* 3, 153–173 (2012).

45. Galiatsatos, P. & Foulkes, W. D. Familial Adenomatous Polyposis. *Am. J. Gastroenterol.* 101, 385–398 (2006).

46. Guinney, J., Dienstmann, R., Wang, X., de Reyniès, A., Schlicker, A., Soneson, C., Marisa, L., Roepman, P., Nyamundanda, G., Angelino, P., Bot, B. M., Morris, J. S., Simon, I. M., Gerster, S., Fessler, E., Melo, F. D. S. E., Missiaglia, E., Ramay, H., Barras, D., Homicsko, K., Maru, D., Manyam, G. C., Broom, B., Boige, V., Perez-Villamil, B., Laderas, T., Salazar, R., Gray, J. W., Hanahan, D., Tabernero, J., Bernards, R., Friend, S. H., Laurent-Puig, P., Medema, J. P., Sadanandam, A., Wessels, L., Delorenzi, M., Kopetz, S., Vermeulen, L. & Tejpar, S. The consensus molecular subtypes of colorectal cancer. *Nat. Med.* advance online publication. (2015).

47. Aaltonen L.A. & Hamilton S.R. World Health Organization Classification of Tumors. Pathology and Genetics of Tumours of the Digestive System. *Lyon Fr. Int. Agency Res. Cancer Press* (2000).

48. Washington, M. K., Powell, A. E., Sullivan, R., Sundberg, J. P., Wright, N., Coffey, R. J. & Dove, W. F. Pathology of Rodent Models of Intestinal Cancer: Progress Report and Recommendations. *Gastroenterology*. 144, 705–717 (2013).

49. Shiga, K., Hara, M., Nagasaki, T., Sato, T., Takahashi, H. & Takeyama, H. Cancer-Associated Fibroblasts: Their Characteristics and Their Roles in Tumor Growth. *Cancers* 7, 2443–2458 (2015).

50. Hawinkels, L. J. A. C., Paauwe, M., Verspaget, H. W., Wiercinska, E., van der Zon, J. M., van der Ploeg, K., Koelink, P. J., Lindeman, J. H. N., Mesker, W., ten Dijke, P. & Sier, C. F. M. Interaction with colon cancer cells hyperactivates TGF-β signaling in cancer-associated fibroblasts. *Oncogene* 33, 97–107 (2014).

51. Powell, D. W., Adegboyega, P. A., Mari, J. F. D. & Mifflin, R. C. Epithelial Cells and Their Neighbors I. Role of intestinal myofibroblasts in development, repair, and cancer. *Am. J. Physiol. Gastrointest. Liver Physiol.* 289, G2–G7 (2005).

52. Smith, N. R., Baker, D., Farren, M., Pommier, A., Swann, R., Wang, X., Mistry, S., McDaid, K., Kendrew, J., Womack, C., Wedge, S. R. & Barry, S. T. Tumor Stromal Architecture Can Define the Intrinsic Tumor Response to VEGF-Targeted Therapy. *Clin. Cancer Res.* 19, 6943–6956 (2013).

53. Lieubeau, B., Garrigue, L., Barbieux, I., Meflah, K. & Gregoire, M. The Role of Transforming Growth Factor β1 in the Fibroblastic Reaction Associated with Rat Colorectal Tumor Development. *Cancer Res.* 54, 6526–6532 (1994).

54. The Cancer Genome Atlas Network, T. C. G. A. N. Comprehensive molecular characterization of human colon and rectal cancer. *Nature* 487, 330–337 (2012).

55. Teglund, S. & Toftgård, R. Hedgehog beyond medulloblastoma and basal cell carcinoma. *Biochim. Biophys. Acta BBA - Rev. Cancer* 1805, 181–208 (2010).

56. Sekulic, A., Migden, M. R., Oro, A. E., Dirix, L., Lewis, K. D., Hainsworth, J. D., Solomon, J. A., Yoo, S., Arron, S. T., Friedlander, P. A., Marmur, E., Rudin, C. M., Chang, A. L. S., Low, J. A., Mackey, H. M., Yauch, R. L., Graham, R. A., Reddy, J. C. & Hauschild, A. Efficacy and safety of vismodegib in advanced basal-cell carcinoma. *N. Engl. J. Med.* 366, 2171–2179 (2012).

57. Yauch, R. L., Gould, S. E., Scales, S. J., Tang, T., Tian, H., Ahn, C. P., Marshall, D., Fu, L., Januario, T., Kallop, D., Nannini-Pepe, M., Kotkow, K., Marsters, J. C., Rubin, L. L. & de Sauvage, F. J. A paracrine requirement for hedgehog signalling in cancer. *Nature* 455, 406–410 (2008).

58. Varnat, F., Duquet, A., Malerba, M., Zbinden, M., Mas, C., Gervaz, P. & Ruiz i Altaba, A. Human colon cancer epithelial cells harbour active HEDGEHOG-GLI signalling that is

essential for tumour growth, recurrence, metastasis and stem cell survival and expansion. *EMBO Mol. Med.* 1, 338–351 (2009).

59. Berlin, J., Bendell, J. C., Hart, L. L., Firdaus, I., Gore, I., Hermann, R. C., Mulcahy, M. F., Zalupski, M. M., Mackey, H. M., Yauch, R. L., Graham, R. A., Bray, G. L. & Low, J. A. A randomized phase II trial of vismodegib versus placebo with FOLFOX or FOLFIRI and bevacizumab in patients with previously untreated metastatic colorectal cancer. *Clin. Cancer Res. Off. J. Am. Assoc. Cancer Res.* 19, 258–267 (2013).

60. Olive, K. P., Jacobetz, M. A., Davidson, C. J., Gopinathan, A., McIntyre, D., Honess, D., Madhu, B., Goldgraben, M. A., Caldwell, M. E., Allard, D., Frese, K. K., DeNicola, G., Feig, C., Combs, C., Winter, S. P., Ireland-Zecchini, H., Reichelt, S., Howat, W. J., Chang, A., Dhara, M., Wang, L., Rückert, F., Grützmann, R., Pilarsky, C., Izeradjene, K., Hingorani, S. R., Huang, P., Davies, S. E., Plunkett, W., Egorin, M., Hruban, R. H., Whitebread, N., McGovern, K., Adams, J., Iacobuzio-Donahue, C., Griffiths, J. & Tuveson, D. A. Inhibition of Hedgehog Signaling Enhances Delivery of Chemotherapy in a Mouse Model of Pancreatic Cancer. *Science* 324, 1457–1461 (2009).

61. Rhim, A. D., Oberstein, P. E., Thomas, D. H., Mirek, E. T., Palermo, C. F., Sastra, S. A., Dekleva, E. N., Saunders, T., Becerra, C. P., Tattersall, I. W., Westphalen, C. B., Kitajewski, J., Fernandez-Barrena, M. G., Fernandez-Zapico, M. E., Iacobuzio-Donahue, C., Olive, K. P. & Stanger, B. Z. Stromal Elements Act to Restrain, Rather Than Support, Pancreatic Ductal Adenocarcinoma. *Cancer Cell* 25, 735–747 (2014).

62. Lee, J. J., Perera, R. M., Wang, H., Wu, D.-C., Liu, X. S., Han, S., Fitamant, J., Jones, P. D., Ghanta, K. S., Kawano, S., Nagle, J. M., Deshpande, V., Boucher, Y., Kato, T., Chen, J. K., Willmann, J. K., Bardeesy, N. & Beachy, P. A. Stromal response to Hedgehog signaling restrains pancreatic cancer progression. *Proc. Natl. Acad. Sci.* 111, E3091–E3100 (2014).

63. Shin, K., Lim, A., Zhao, C., Sahoo, D., Pan, Y., Spiekerkoetter, E., Liao, J. C. & Beachy, P. A. Hedgehog Signaling Restrains Bladder Cancer Progression by Eliciting Stromal Production of Urothelial Differentiation Factors. *Cancer Cell* 26, 521–533 (2014).

64. Moser, A. R., Pitot, H. C. & Dove, W. F. A dominant mutation that predisposes to multiple intestinal neoplasia in the mouse. *Science* 247, 322–324 (1990).

65. Johnson, R. L. & Fleet, J. C. Animal Models of Colorectal Cancer. *Cancer Metastasis Rev.* 32, 39–61 (2013).

66. Neufert, C., Becker, C. & Neurath, M. F. An inducible mouse model of colon carcinogenesis for the analysis of sporadic and inflammation-driven tumor progression. *Nat. Protoc.* 2, 1998–2004 (2007).

67. Boivin, G. P., Washington, K., Yang, K., Ward, J. M., Pretlow, T. P., Russell, R., Besselsen, D. G., Godfrey, V. L., Doetschman, T., Dove, W. F., Pitot, H. C., Halberg, R. B., Itzkowitz, S. H., Groden, J. & Coffey, R. J. Pathology of mouse models of intestinal cancer: Consensus report and recommendations. *Gastroenterology* 124, 762–777 (2003).

68. Naylor, L. H. Reporter gene technology: the future looks bright. *Biochem. Pharmacol.* 58, 749–757 (1999).

69. Bai, C. B., Auerbach, W., Lee, J. S., Stephen, D. & Joyner, A. L. Gli2, but not Gli1, is required for initial Shh signaling and ectopic activation of the Shh pathway. *Development* 129, 4753–4761 (2002).

70. Sternberg, N. & Hamilton, D. Bacteriophage P1 site-specific recombination: I. Recombination between loxP sites. *J. Mol. Biol.* 150, 467–486 (1981).

71. Feil, S., Valtcheva, N. & Feil, R. Inducible Cre mice. *Methods Mol. Biol.* (Clifton NJ). 530, 343–363 (2009).

72. Kasper, M., Jaks, V., Are, A., Bergström, Å., Schwäger, A., Svärd, J., Teglund, S., Barker, N. & Toftgård, R. Wounding enhances epidermal tumorigenesis by recruiting hair follicle keratinocytes. *Proc. Natl. Acad. Sci. U. S. A.* 108, 4099–4104 (2011).

73. Zheng, B., Zhang, Z., Black, C. M., de Crombrugghe, B. & Denton, C. P. Ligand-Dependent Genetic Recombination in Fibroblasts: A Potentially Powerful Technique for Investigating Gene Function in Fibrosis. *Am. J. Pathol.* 160, 1609–1617 (2002).

74. Madisen, L., Zwingman, T. A., Sunkin, S. M., Oh, S. W., Zariwala, H. A., Gu, H., Ng, L. L., Palmiter, R. D., Hawrylycz, M. J., Jones, A. R., Lein, E. S. & Zeng, H. A robust and high-throughput Cre reporting and characterization system for the whole mouse brain. *Nat. Neurosci.* 13, 133–140 (2010).

75. Chung, J. H. & Bunz, F. A loss-of-function mutation in PTCH1 suggests a role for autocrine hedgehog signaling in colorectal tumorigenesis. *Oncotarget* 4, 2208–2211 (2013).

76. Mazumdar, T., DeVecchio, J., Shi, T., Jones, J., Agyeman, A. & Houghton, J. A. Hedgehog Signaling Drives Cellular Survival in Human Colon Carcinoma Cells. *Cancer Res.* 71, 1092–1102 (2011).

77. Yauch, R. L., Gould, S. E., Scales, S. J., Tang, T., Tian, H., Ahn, C. P., Marshall, D., Fu, L., Januario, T., Kallop, D., Nannini-Pepe, M., Kotkow, K., Marsters, J. C., Rubin, L. L. & de Sauvage, F. J. A paracrine requirement for hedgehog signalling in cancer. *Nature* 455, 406–410 (2008).

78. Ahn, S. & Joyner, A. L. Dynamic changes in the response of cells to positive hedgehog signaling during mouse limb patterning. *Cell* 118, 505–516 (2004).

79. Gerling, M., Büller, N. V. J. A., Kirn, L. M., Joost, S., Frings, O., Englert, B., Bergström, Å., Kuiper, R. V., Blaas, L., Wielenga, M. C. B., Almer, S., Kühl, A. A., Fredlund, E., van den Brink, G. R. & Toftgård, R. Stromal Hedgehog signalling is downregulated in colon cancer and its restoration restrains tumour growth. *Nat. Commun.* 7, 12321 (2016).

80. Gerling, M., Zhao, Y., Nania, S., Norberg, K. J., Verbeke, C. S., Englert, B., Kuiper, R. V., Bergström, Å., Hassan, M., Neesse, A., Löhr, J. M. & Heuchel, R. L. Real-Time Assessment of Tissue Hypoxia In Vivo with Combined Photoacoustics and High-Frequency Ultrasound. *Theranostics* 4, 604–613 (2014).

81. Glasel, J. A. Validity of nucleic acid purities monitored by 260nm/280nm absorbance ratios. *BioTechniques* 18, 62–63 (1995).

82. Zipper, H., Brunner, H., Bernhagen, J. & Vitzthum, F. Investigations on DNA intercalation and surface binding by SYBR Green I, its structure determination and methodological implications. *Nucleic Acids Res.* 32, e103 (2004).

83. Schefe, J. H., Lehmann, K. E., Buschmann, I. R., Unger, T. & Funke-Kaiser, H. Quantitative real-time RT-PCR data analysis: current concepts and the novel 'gene expression's CT difference' formula. *J. Mol. Med.* 84, 901–910 (2006).

84. Schena, M., Shalon, D., Davis, R. W. & Brown, P. O. Quantitative Monitoring of Gene Expression Patterns with a Complementary DNA Microarray. *Science* 270, 467–470 (1995).

85. Subramanian, A., Tamayo, P., Mootha, V. K., Mukherjee, S., Ebert, B. L., Gillette, M. A., Paulovich, A., Pomeroy, S. L., Golub, T. R., Lander, E. S. & Mesirov, J. P. Gene set enrichment analysis: A knowledge-based approach for interpreting genome-wide expression profiles. *Proc. Natl. Acad. Sci.* 102, 15545–15550 (2005).

86. Edgar, R., Domrachev, M. & Lash, A. E. Gene Expression Omnibus: NCBI gene expression and hybridization array data repository. *Nucleic Acids Res.* 30, 207–210 (2002).

87. Chen, W., Tang, T., Eastham-Anderson, J., Dunlap, D., Alicke, B., Nannini, M., Gould, S., Yauch, R., Modrusan, Z., DuPree, K. J., Darbonne, W. C., Plowman, G., Sauvage, F. J. de & Callahan, C. A. Canonical hedgehog signaling augments tumor angiogenesis by induction of VEGF-A in stromal perivascular cells. *Proc. Natl. Acad. Sci.* 108, 9589–9594 (2011).

88. Gautier, L., Cope, L., Bolstad, B. M. & Irizarry, R. A. affy—analysis of Affymetrix GeneChip data at the probe level. *Bioinformatics* 20, 307–315 (2004).

89. Ritchie, M. E., Phipson, B., Wu, D., Hu, Y., Law, C. W., Shi, W. & Smyth, G. K. limma powers differential expression analyses for RNA-sequencing and microarray studies. *Nucleic Acids Res.* 43, e47 (2015).

90. Benjamini, Y. & Hochberg, Y. Controlling The False Discovery Rate - A Practical And Powerful Approach To Multiple Testing. *J. R. Stat. Soc. Ser. B Methodol.* 57, No. 1, 289–300 (1995).

91. Fazio, V., Robertis, M., Massi, E., Poeta, M., Carotti, S., Morini, S., Cecchetelli, L. & Signori, E. The AOM/DSS murine model for the study of colon carcinogenesis: From pathways to diagnosis and therapy studies. *J. Carcinog.* 10, 9 (2011).

92. Snippert, H. J., Schepers, A. G., Delconte, G., Siersema, P. D. & Clevers, H. Slide preparation for single-cell-resolution imaging of fluorescent proteins in their three-dimensional near-native environment. *Nat. Protoc.* 6, 1221–1228 (2011).

93. Wiener, Z., Högström, J., Hyvönen, V., Band, A. M., Kallio, P., Holopainen, T., Dufva, O., Haglund, C., Kruuna, O., Oliver, G., Ben-Neriah, Y. & Alitalo, K. Prox1 Promotes Expansion of the Colorectal Cancer Stem Cell Population to Fuel Tumor Growth and Ischemia Resistance. *Cell Rep.* 8, 1943–1956 (2014).

94. Farrall, A. L., Riemer, P., Leushacke, M., Sreekumar, A., Grimm, C., Herrmann, B. G. & Morkel, M. Wnt and BMP signals control intestinal adenoma cell fates. *Int. J. Cancer* 131, 2242–2252 (2012).

95. Lombardo, Y., Scopelliti, A., Cammareri, P., Todaro, M., Iovino, F., Ricci–Vitiani, L., Gulotta, G., Dieli, F., de Maria, R. & Stassi, G. Bone Morphogenetic Protein 4 Induces Differentiation of Colorectal Cancer Stem Cells and Increases Their Response to Chemotherapy in Mice. *Gastroenterology* 140, 297–309.e6 (2011).

96. Büller, N. V. J. A., Rosekrans, S. L., Metcalfe, C., Heijmans, J., van Dop, W. A., Fessler, E., Jansen, M., Ahn, C., Vermeulen, J. L. M., Westendorp, B. F., Robanus-Maandag, E. C., Offerhaus, G. J., Medema, J. P., D'Haens, G. R. A. M., Wildenberg, M. E., de Sauvage, F. J., Muncan, V. & van den Brink, G. R. Stromal Indian hedgehog signaling is required for intestinal adenoma formation in mice. *Gastroenterology* 148, 170–180.e6 (2015).

97. Liem, K. F., Jessell, T. M. & Briscoe, J. Regulation of the neural patterning activity of sonic hedgehog by secreted BMP inhibitors expressed by notochord and somites. *Development* 127, 4855–4866 (2000).

98. Herter-Sprie, G. S., Kung, A. L. & Wong, K. K. New cast for a new era: preclinical cancer drug development revisited. *J. Clin. Invest.* 123, 3639–3645 (2013).

99. Corpet, D. E. & Pierre, F. How good are rodent models of carcinogenesis in predicting efficacy in humans? A systematic review and meta-analysis of colon chemoprevention in rats, mice and men. *Eur. J. Cancer* 41, 1911–1922 (2005).

100. Takahashi, M., Nakatsugi, S., Sugimura, T. & Wakabayashi, K. Frequent mutations of the beta-catenin gene in mouse colon tumors induced by azoxymethane. *Carcinogenesis* 21, 1117–1120 (2000).

101. Fazio, V., Robertis, M., Massi, E., Poeta, M., Carotti, S., Morini, S., Cecchetelli, L. & Signori, E. The AOM/DSS murine model for the study of colon carcinogenesis: From pathways to diagnosis and therapy studies. *J. Carcinog.* 10, 9 (2011).

102. Tanaka, T., Kohno, H., Suzuki, R., Yamada, Y., Sugie, S. & Mori, H. A novel inflammation-related mouse colon carcinogenesis model induced by azoxymethane and dextran sodium sulfate. *Cancer Sci.* 94, 965–973 (2003).

103. Munkholm, P. Review article: the incidence and prevalence of colorectal cancer in inflammatory bowel disease. *Aliment. Pharmacol. Ther.* 18, 1–5 (2003).

104. Kobaek-Larsen, M., Thorup, I., Diederichsen, A., Fenger, C. & Hoitinga, M. R. Review of Colorectal Cancer and Its Metastases in Rodent Models: Comparative Aspects with Those in Humans. *Comp. Med.* 50, 16–26 (2000).

105. Leong, A.-Y. & Wright, J. The contribution of immunohistochemical staining in tumour diagnosis. *Histopathology* 11, 1295–1305 (1987).

106. de Matos, L. L., Trufelli, D. C., de Matos, M. G. L. & da Silva Pinhal, M. A. Immunohistochemistry as an Important Tool in Biomarkers Detection and Clinical Practice. *Biomark Insights* 5, 9–20 (2010).

107. Nolan, T., Hands, R. E. & Bustin, S. A. Quantification of mRNA using real-time RT-PCR. *Nat. Protoc.* 1, 1559–1582 (2006).

108. Rubie, C., Kempf, K., Hans, J., Su, T., Tilton, B., Georg, T., Brittner, B., Ludwig, B. & Schilling, M. Housekeeping gene variability in normal and cancerous colorectal, pancreatic, esophageal, gastric and hepatic tissues. *Mol. Cell. Probes* 19, 101–109 (2005).

109. Akamine, R., Yamamoto, T., Watanabe, M., Yamazaki, N., Kataoka, M., Ishikawa, M., Ooie, T., Baba, Y. & Shinohara, Y. Usefulness of the 5′ region of the cDNA encoding acidic ribosomal phosphoprotein P0 conserved among rats, mice, and humans as a standard probe for gene expression analysis in different tissues and animal species. *J. Biochem. Biophys. Methods* 70, 481–486 (2007).

110. Krzystek-Korpacka, M., Diakowska, D., Bania, J. & Gamian, A. Expression Stability of Common Housekeeping Genes Is Differently Affected by Bowel Inflammation and Cancer: Implications for Finding Suitable Normalizers for Inflammatory Bowel Disease Studies. *Inflamm. Bowel Dis.* 20, 1147–1156 (2014).

111. Lockhart, D. J., Dong, H., Byrne, M. C., Follettie, M. T., Gallo, M. V., Chee, M. S., Mittmann, M., Wang, C., Kobayashi, M., Norton, H. & Brown, E. L. Expression monitoring

by hybridization to high-density oligonucleotide arrays. *Nat. Biotechnol.* 14, 1675–1680 (1996).

112. Okoniewski, M. J. & Miller, C. J. Hybridization interactions between probesets in short oligo microarrays lead to spurious correlations. *BMC Bioinformatics* 7, 276 (2006).

113. Rubin, L. L. & de Sauvage, F. J. Targeting the Hedgehog pathway in cancer. *Nat. Rev. Drug Discov.* 5, 1026–1033 (2006).

114. Kolterud, Å., Grosse, A. S., Zacharias, W. J., Walton, K. D., Kretovich, K. E., Madison, B. B., Waghray, M., Ferris, J. E., Hu, C., Merchant, J. L., Dlugosz, A. A., Kottmann, A. H. & Gumucio, D. L. Paracrine Hedgehog Signaling in Stomach and Intestine: New Roles for Hedgehog in Gastrointestinal Patterning. *Gastroenterology* 137, 618–628 (2009).

115. Varnat, F., Duquet, A., Malerba, M., Zbinden, M., Mas, C., Gervaz, P. & Ruiz i Altaba, A. Human colon cancer epithelial cells harbour active HEDGEHOG-GLI signalling that is essential for tumour growth, recurrence, metastasis and stem cell survival and expansion. *EMBO Mol. Med.* 1, 338–351 (2009).

116. Scales, S. J. & de Sauvage, F. J. Mechanisms of Hedgehog pathway activation in cancer and implications for therapy. *Trends Pharmacol. Sci.* 30, 303–312 (2009).

117. Lee, J. J., Rothenberg, M. E., Seeley, E. S., Zimdahl, B., Kawano, S., Lu, W.-J., Shin, K., Sakata-Kato, T., Chen, J. K., Diehn, M., Clarke, M. F. & Beachy, P. A. Control of inflammation by stromal Hedgehog pathway activation restrains colitis. *Proc. Natl. Acad. Sci.* 113, E7545–E7553 (2016).

118. Cohen, M., Kicheva, A., Ribeiro, A., Blassberg, R., Page, K. M., Barnes, C. P. & Briscoe, J. Ptch1 and Gli regulate Shh signalling dynamics via multiple mechanisms. *Nat. Commun.* 6, (2015).

119. Sadanandam, A., Lyssiotis, C. A., Homicsko, K., Collisson, E. A., Gibb, W. J., Wullschleger, S., Ostos, L. C. G., Lannon, W. A., Grotzinger, C., Del Rio, M., Lhermitte, B., Olshen, A.

B., Wiedenmann, B., Cantley, L. C., Gray, J. W. & Hanahan, D. A colorectal cancer classification system that associates cellular phenotype and responses to therapy. *Nat. Med.* 19, 619–625 (2013).

120. Thibert, C., Teillet, M.-A., Lapointe, F., Mazelin, L., Douarin, N. M. L. & Mehlen, P. Inhibition of Neuroepithelial Patched-Induced Apoptosis by Sonic Hedgehog. *Science* 301, 843–846 (2003).

121. Bredesen, D. E., Mehlen, P. & Rabizadeh, S. Apoptosis and Dependence Receptors: A Molecular Basis for Cellular Addiction. *Physiol. Rev.* 84, 411–430 (2004).

122. Shyer, A. E., Huycke, T. R., Lee, C., Mahadevan, L. & Tabin, C. J. Bending Gradients: How the Intestinal Stem Cell Gets Its Home. *Cell* 161, 569–580 (2015).

123. Li, X., Nadauld, L., Ootani, A., Corney, D. C., Pai, R. K., Gevaert, O., Cantrell, M. A., Rack, P. G., Neal, J. T., Chan, C. W.-M., Yeung, T., Gong, X., Yuan, J., Wilhelmy, J., Robine, S., Attardi, L. D., Plevritis, S. K., Hung, K. E., Chen, C.-Z., Ji, H. P. & Kuo, C. J. Oncogenic transformation of diverse gastrointestinal tissues in primary organoid culture. *Nat. Med.* 20, 769-777 (2014).

124. Büller, N. V. J. A., Rosekrans, S. L., Metcalfe, C., Heijmans, J., van Dop, W. A., Fessler, E., Jansen, M., Ahn, C., Vermeulen, J. L. M., Westendorp, B. F., Robanus-Maandag, E. C., Offerhaus, G. J., Medema, J. P., D'Haens, G. R. A. M., Wildenberg, M. E., de Sauvage, F. J., Muncan, V. & van den Brink, G. R. Stromal Indian Hedgehog Signaling Is Required for Intestinal Adenoma Formation in Mice. *Gastroenterology* 148, 170–180.e6 (2015).

125. He, X. C., Zhang, J., Tong, W.-G., Tawfik, O., Ross, J., Scoville, D. H., Tian, Q., Zeng, X., He, X., Wiedemann, L. M., Mishina, Y. & Li, L. BMP signaling inhibits intestinal stem cell self-renewal through suppression of Wnt–β-catenin signaling. *Nat. Genet.* 36, 1117–1121 (2004).

126. Kawai, S. & Sugiura, T. Characterization of human bone morphogenetic protein (BMP)-4 and -7 gene promoters: activation of BMP promoters by Gli, a sonic hedgehog mediator1. *Bone* 29, 54–61 (2001).

127. Howe, J. R., Bair, J. L., Sayed, M. G., Anderson, M. E., Mitros, F. A., Petersen, G. M., Velculescu, V. E., Traverso, G. & Vogelstein, B. Germline mutations of the gene encoding bone morphogenetic protein receptor 1A in juvenile polyposis. *Nat. Genet.* 28, 184–187 (2001).

128. Jaeger, E., Webb, E., Howarth, K., Carvajal-Carmona, L., Rowan, A., Broderick, P., Walther, A., Spain, S., Pittman, A., Kemp, Z., Sullivan, K., Heinimann, K., Lubbe, S., Domingo, E., Barclay, E., Martin, L., Gorman, M., Chandler, I., Vijayakrishnan, J., Wood, W., Papaemmanuil, E., Penegar, S., Qureshi, M., Farrington, S., Tenesa, A., Cazier, J.-B., Kerr, D., Gray, R., Peto, J., Dunlop, M., Campbell, H., Thomas, H., Houlston, R. & Tomlinson, I. Common genetic variants at the CRAC1 (HMPS) locus on chromosome 15q13.3 influence colorectal cancer risk. *Nat. Genet.* 40, 26–28 (2008).

129. Eppig, J. T. in *Mouse Biomed. Res. Second Ed.* (eds. Fox, J. G., Davisson, M. T., Quimby, F. W., Barthold, S. W., Newcomer, C. E. & Smith, A. L.) 79–98 (Academic Press, 2007).

130. Wain, H. M., Bruford, E. A., Lovering, R. C., Lush, M. J., Wright, M. W. & Povey, S. Guidelines for human gene nomenclature. *GENOMICS* 79, 464–470 (2002).

9 Abbreviations

AOM	Azoxymethane
APC	Adenomatous polyposis coli
BAMBI	BMP and activin membrane-bound inhibitor homologue
BMP	Bone Morphogenetic Protein
CAF	Cancer-associated fibroblast
cDNA	Complementary DNA
CEA	Carcinoembryonic antigen
CMS	Consensus molecular subtypes
Chrd	Chordin
Col1a2	Collagen1a2
CRC	Colorectal cancer
CRDL1	Chordin-like 1
Cre	Cyclic recombinase
CreERT	Cre-proteins with tamoxifen-inducible domains
CSFG	Cold fish skin gelatin
DAB	3,3´-Diaminobenzidine
DCC	Deleted in colorectal carcinoma
DHH	Desert Hedgehog
DISP	Dispatched
DNA	Deoxyribonucleic Acid
dNTP	Deoxynucleoside triphosphate
DSS	Dextran sodium sulfate
dT	Deoxythymidylic Deoxythymidylic acid
ECM	Extracellular matrix
FAP	Familial adenomatous polyposis
FAPα	Fibroblast-activation protein α
GEO	Gene expression omnibus
GLI	Glioma-associated protein homologue
GREM1	Gremlin 1
GREM2	Gremlin 2
GSEA	Gene set enrichment analysis
Hh	Hedgehog

HHIP	Hedgehog-interacting protein
HNPCC	Hereditary nonpolyposis colorectal cancer (or Lynch-Syndrome)
IF	Immunofluorescence
IHC	Immunohistochemistry
IHH	Indian Hedgehog
IL-6	Interleukin 6
ISEMF	Intestinal subepithelial myofibroblast
LacZ	Gene of the lac operon encoding for beta-galactosidase lactose Z
LEF	Lymphocyte enhancer factor
Lgr5	Leucine-rich-repeat-containing G protein-coupled receptor 5
LoxP	Locus of Crossover in P1
Min	Multiple intestinal neoplasia
mRNA	Messenger Ribonucleic Acid
MSC	Mesenchymal stem cells
MSigDB	Molecular signature data base
Nog	Noggin
PBS	Phosphate buffered saline
PDAC	Pancreatic ductal adenocarcinoma
PROX1	Prospero homeobox 1
p-Smad	Phosphorylated-Smad
PTCH	Patched
RNA	Ribonucleic acid
RPLP0/ARP	Ribosomal protein, large, P0/ acidic ribosomal protein
R-Smad	Receptor-associated Smad
RT-qPCR	Real-time quantitative polymerase chain reaction
SEM	Standard error of the means
SHH	Sonic Hedgehog
Smad	Sma and Mad (Mothers gainst decapentaplegic)
SMO	Smoothened
TGF-β	Transforming growth factor-β
TCF	T cell factor
wt	Wild type
α-SMA	α-smooth muscle actin

Gene, protein and mRNA symbols are abbreviated and italicized according to the conventional nomenclature [129,130] as follows:

Species	Gene Symbol	Protein Symbol	mRNA
Homo Sapiens	*SHH*	SHH	*SHH*
Mus muculus	*Shh*	SHH	*Shh*

10 Eidesstattliche Versicherung

„Ich, **Leonard Kirn**, versichere an Eides statt durch meine eigenhändige Unterschrift, dass ich die vorgelegte Dissertation mit dem Thema**: Tumor-Stroma Crosstalk in Colorectal Cancer: The Role of Paracrine Hedgehog Signaling** selbstständig und ohne nicht offengelegte Hilfe Dritter verfasst und keine anderen als die angegebenen Quellen und Hilfsmittel genutzt habe.

Alle Stellen, die wörtlich oder dem Sinne nach auf Publikationen oder Vorträgen anderer Autoren beruhen, sind als solche in korrekter kenntlich gemacht. Die Abschnitte zu Methodik und Resultaten entsprechen den Uniform Requirements for Manuscripts (URM) und werden von mir verantwortet.
Meine Anteile an etwaigen Publikationen zu dieser Dissertation entsprechen denen, die in der untenstehenden gemeinsamen Erklärung mit dem Betreuer, angegeben sind. Sämtliche Publikationen, die aus dieser Dissertation hervorgegangen sind und bei denen ich Autor bin, entsprechen den URM und werden von mir verantwortet.

Die Bedeutung dieser eidesstattlichen Versicherung und die strafrechtlichen Folgen einer unwahren eidesstattlichen Versicherung (§156,161 des Strafgesetzbuches) sind mir bekannt und bewusst.“

Datum Unterschrift

11 Anteilserklärung

Leonard Kirn hatte folgenden Anteil an der folgenden Publikation:

Marco Gerling, Nike V.J.A. Büller*, Leonard M. Kirn*, Simon Joost, Oliver Frings, Benjamin Englert, Åsa Bergström, Raoul V. Kuiper, Leander Blaas, Mattheus C.B. Wielenga, Sven Almer, Anja A. Kühl, Erik Fredlund, Gijs R. van den Brink & Rune Toftgård (2016). *Stromal Hedgehog signalling is downregulated in colon cancer and its restoration restrains tumour growth*. Nature Communications *7*, 12321; doi:10.1038/ncomms12321; *geteilte Zweitautorenschaft

Beitrag im Einzelnen:

- RNA Extraktion und PCR (praktisch und Auswertung)
    - Durch die von mir praktisch durchgeführte RNA Extraktion und PCR, sowie deren Auswertung sind die Graphen 1e, 2d, 4d und 5g entstanden.
- IHC und IF (praktisch und Auswertung)
    - Durch die von mir durchgeführten IHC und IF, sowie deren Auswertungen sind folgende Abbildungen entstanden: 1g, 1h, 3 (in Teilen) und 6e, f und h
- Assistenz bei der Durchführung von Tierexperimenten
    - Behandlung mit AOM und DSS sowie Tamoxifen, Analyse des gesundheitlichen Status, Euthanasie und Sezernierung (für Teile der Experimente in Abbildung 1 a-c, 3 und 4 a-d)
- Verfassen von Teilen der Methoden des Manuskriptes
- Korrekturlesen des Hauptteils des Manuskriptes

Unterschrift, Datum und Stempel des betreuenden Hochschullehrers/der betreuenden Hochschullehrerin

Unterschrift des Doktoranden/der Doktorandin

12 Lebenslauf

Mein Lebenslauf wird aus datenschutzrechtlichen Gründen in der elektronischen Version meiner Arbeit nicht veröffentlicht.

Mein Lebenslauf wird aus datenschutzrechtlichen Gründen in der elektronischen Version meiner Arbeit nicht veröffentlicht.

13 Publikationsliste

Marco Gerling, Nike V.J.A. Büller*, Leonard M. Kirn*, Simon Joost, Oliver Frings, Benjamin Englert, Åsa Bergström, Raoul V. Kuiper, Leander Blaas, Mattheus C.B. Wielenga, Sven Almer, Anja A. Kühl, Erik Fredlund, Gijs R. van den Brink & Rune Toftgård (2016). *Stromal Hedgehog signalling is downregulated in colon cancer and its restoration restrains tumour growth*. Nature Communications *7*, 12321; doi:10.1038/ncomms12321; * equal contribution

14 Danksagung

Ich möchte mich ganz herzlich bei meiner Doktormutter Frau Prof. Dr. Britta Siegmund für die exzellente Betreuung bedanken. Auch möchte ich mich dafür bedanken, dass sie es mir ermöglicht hat, einen Teil meiner Arbeit im Ausland zu absolvieren. Ihr kompetenter Rat und ihre Unterstützung haben mir sehr geholfen.

Herrn Prof. Rune Toftgård danke ich für die sehr freundliche Aufnahme in seine Arbeitsgruppe am Karolinska Institut, Stockholm und das Bereitstellen der Mausproben, des Arbeitsplatzes und der Chemikalien. Bei der gesamten Arbeitsgruppe möchte ich mich für die sehr warmherzige Aufnahme, die vielen Hilfestellungen und die unvergesslichen *Fikas* bedanken.
Für die Unterstützung mit der Informatik und mit der Statistik möchte ich Simon Joost besonders danken, welcher für mich auch die Gene Expression Omnibus (GEO) Daten analysiert hat. Bei Benjamin Englert möchte ich mich ganz herzlich für die Unterstützung bei den PCR Analysen und seinen Hilfestellungen mit den Mausmodellen bedanken.
Bei der Böhringer Ingelheim Stiftung möchte ich mich für die finanzielle Unterstützung und die herzliche Aufnahme in ihr Stipendienprogramm bedanken, die mir meinen Forschungsaufenthalt mit ermöglicht haben.

Mein ganz besonderer Dank geht an Herrn Dr. Marco Gerling, der mich über die gesamte Dauer mit einer beeindruckenden Geduld unterstützt hat, mich wunderbar in das Team in Stockholm integriert hat und jederzeit ein Ohr für meine Wünsche und Fragen hatte. Ich hätte mir keine bessere Begleitung während der letzten Jahre vorstellen können.

Auch möchte ich mich bei all meinen super Freunden für die schönen Kaffeepausen bedanken, die mir jedes Mal ein wenig Energie gespendet haben.

Abschließend will ich mich bei meinen Eltern und meinen Geschwistern, Johannes und Marcia, bedanken, die mich mein Leben lang mit einer unbeschreiblichen Liebe unterstützt haben.